

Efficient Direct-Connect Topologies for Collective Communications

Liangyu Zhao
Univ. of Washington

Siddharth Pal
Raytheon BBN

Tapan Chugh
Univ. of Washington

Weiyang Wang
MIT CSAIL

Prithwish Basu
Raytheon BBN

Joud Khoury
Raytheon BBN

Arvind Krishnamurthy
Univ. of Washington

Abstract

We consider the problem of distilling efficient network topologies for collective communications. We provide an algorithmic framework for constructing direct-connect topologies optimized for the node latency vs bandwidth trade-off given a collective communication workload. Our algorithmic framework allows us to start from small base topologies and associated communication schedules and use a set of techniques that can be iteratively applied to derive much larger topologies. The schedules for these derived topologies are either synthesized along with the expansions or computed using an optimization formulation. Our approach allows us to synthesize many different topologies and schedules for a given cluster size and degree, and then identify the appropriate topology and schedule for a given workload. We evaluate our approach on a 12-node optical testbed that uses patch panels for configuring the desired topology and augment it with an analytical-model-based evaluation for larger deployments. We show that the derived topologies and schedules provide significant performance benefits over existing approaches.

1 Introduction

Collective communication operations have received significant attention in both machine learning (ML) and high-performance computing (HPC) disciplines. These operations involve concurrently aggregating and distributing data on a cluster of nodes. These primitives are not only frequently used but are often the primary source of communication costs. Indeed recent works suggest that with the explosive growth in the size of models and improved computational capabilities, the collective operations for parameter synchronization across GPUs have become a significant source of overhead in large scale distributed ML training [30, 57, 68].

An emerging approach to meet these challenging demands has been to employ various forms of optical circuit switching to achieve higher bandwidths at reasonable capital expenditure and energy costs [40, 45, 64, 69, 77]. Hosts communicate

using a limited number of optical circuits that can be reconfigured (at timescales appropriate for the hardware), thus exposing network topology as a configurable component. At the same time, reconfiguration times of today's fastest commercially available optical circuits are still on the order of several milliseconds [23, 24, 54, 61, 77], which is high compared to the total time to complete the collective operation (e.g., order of milliseconds for a typical DNN layer over 100 Gbps links). Given these high reconfiguration costs, collectives need to operate over a set of pre-configured circuits that remain unchanged. We refer to this setting as *direct-connect*, circuits that are configured and remain static, at least for the duration of the collective algorithm.

Existing optical circuits-based ML systems fit this direct-connect model and can adopt only those collective algorithms whose communication patterns satisfy the degree constraints of the optical fabric (e.g., rings, multi-rings, tori, and trees with bounded degree) [40, 45, 64, 77] and accept the inherent tradeoffs associated with them. For example, collective communications over a ring, while bandwidth-efficient, have high node latency as messages must travel around the ring, and a double binary tree has logarithmic node latency but suffers from load imbalances and bandwidth inefficiencies. The broader spectrum of well-known collective algorithms that achieve desired latency and bandwidth properties (e.g., recursive-doubling, Bruck algorithm) [63, 71] cannot be utilized given their "high-degree" communication patterns. Such algorithms are not amenable to efficient implementation even on research prototypes of fast reconfigurable optical circuits [11, 47, 55, 70] that are demand-agnostic and aim to deliver uniform all-to-all bandwidth.

To fill this gap, we seek to identify new topologies and communication schedules that are customized for direct-connect networks. We pose the following research question: *Can we efficiently determine high-performance direct-connect topologies and communication schedules for collectives given the constraints of the optical fabric and the target workload?*

Several challenges need to be tackled in addressing this research question. First, we seek to distill *both* the network

topology and the communications schedule appropriate for the topology, which is unlike other efforts that focus on one or the other (e.g., schedules for a given network [18, 58, 68] or topology permutations for a given ring schedule [69]). Finding a topology and communications schedule for small low-degree networks is tractable. But, at a large scale, the combination of topological structure and communications schedule as degrees of freedom explodes the search space, making this a seemingly intractable problem. Current state-of-the-art approaches do not have a way of handling this complex joint optimization problem. Second, collective communications can be both latency- and bandwidth-sensitive depending on the workload and the performance of the low-level communication primitives. A network topology has to balance the need for minimizing the number of hops associated with performing the collective with load imbalances incurred on specific network links. Finally, lowering the synthesized schedules to the underlying GPU and communication runtimes [37, 48] in an efficient way requires careful scheduling to achieve desired performance in practice.

Our work addresses these issues by developing an algorithmic toolchain for quickly synthesizing efficient topologies and schedules for collective communications. We make the following contributions to achieve this goal.

- (1) **Algorithmic framework for synthesizing network topologies:** We start with small base graphs that have optimal performance for collectives (e.g., well-known *regular graphs* of uniform degree and custom-built graphs). We design different graph expansion techniques to construct larger graphs of the desired degree while almost preserving the latency and bandwidth properties of the base graphs.
- (2) **Efficient computation of communication schedules:** The communication schedules for the expanded graphs are synthesized along with the expansions. We also develop a linear program to compute high-performance schedules for large-scale topologies from graph theory, thereby avoiding generating schedules through NP-hard discrete optimization.
- (3) **Topology enumeration and search:** We enumerate the *Pareto-efficient* options that provide different trade-offs for bandwidth and latency, and identify the appropriate option for a target cluster and workload.
- (4) **Efficient code generation for GPUs:** We build a general compiler for lowering our mathematically expressed schedules to the MSCCL runtime [48], which integrates into many popular training frameworks such as PyTorch.

We evaluate using an optical patch panel [39, 62, 69], a mechanical reconfiguration solution that is cheaper and has a higher port count than optical circuit switches. For DNN workloads, the derived topologies and schedules provide significant benefits over baseline approaches on the small testbed (30% and 50% faster than the most competitive bandwidth-optimizing and latency-sensitive topology+schedule,

respectively). More significant gains are observed at a larger scale (1024 GPUs) via simulations: our topologies+schedules are on average 73× and 25× faster than bandwidth-optimal and latency-sensitive baselines, respectively.

2 Model and Background

Before			After		
Reduce-Scatter					
Node 0	Node 1	Node 2	Node 0	Node 1	Node 2
$S_0^{(0)}$	$S_0^{(1)}$	$S_0^{(2)}$	$\oplus_i S_0^{(i)}$	$\oplus_i S_1^{(i)}$	$\oplus_i S_2^{(i)}$
$S_1^{(0)}$	$S_1^{(1)}$	$S_1^{(2)}$			
$S_2^{(0)}$	$S_2^{(1)}$	$S_2^{(2)}$			
Allgather					
Node 0	Node 1	Node 2	Node 0	Node 1	Node 2
$S_0^{(0)}$	$S_1^{(1)}$	$S_2^{(2)}$	$S_0^{(0)}$	$S_0^{(0)}$	$S_0^{(0)}$
			$S_1^{(1)}$	$S_1^{(1)}$	$S_1^{(1)}$
			$S_2^{(2)}$	$S_2^{(2)}$	$S_2^{(2)}$
Allreduce					
Node 0	Node 1	Node 2	Node 0	Node 1	Node 2
$S_0^{(0)}$	$S_0^{(1)}$	$S_0^{(2)}$	$\oplus_i S_0^{(i)}$	$\oplus_i S_0^{(i)}$	$\oplus_i S_0^{(i)}$
$S_1^{(0)}$	$S_1^{(1)}$	$S_1^{(2)}$	$\oplus_i S_1^{(i)}$	$\oplus_i S_1^{(i)}$	$\oplus_i S_1^{(i)}$
$S_2^{(0)}$	$S_2^{(1)}$	$S_2^{(2)}$	$\oplus_i S_2^{(i)}$	$\oplus_i S_2^{(i)}$	$\oplus_i S_2^{(i)}$

Table 1: The state before and after the collective communications. $S_j^{(i)}$ denotes the j -th shard of data at node i . In particular, the size of each $S_j^{(i)}$ is $|S_j^{(i)}| = M/N$. The operator \oplus is the reduction operator (e.g., sum).

We focus on three collective communication operations: **reduce-scatter**, **allgather**, and **allreduce**. N nodes perform a collective operation on a vector of data (or model) of total size M . Prior to the operation, each node i possesses a vector of data that can be split into N shards, where $S_j^{(i)}$ denotes the j -th shard of data at node i . Table 1 shows an example of how three nodes perform all three collectives. In *reduce-scatter*, each node i reduces the i -th shard from all other nodes; in *allgather*, each node i broadcasts the i -th shard to all other nodes; in *allreduce*, each node i ends up with the fully reduced vector of data.

Throughout the paper, we only elaborate on the *reduce-scatter* topologies and schedules because the other two collectives are direct transformations. Specifically, to construct the *allgather* schedule, we simply reverse the communications in the *reduce-scatter* [20] (§A). To construct the *allreduce* algorithm, we concatenate the *reduce-scatter* schedule with the *allgather* schedule. Thus, *allgather* has the same runtime, and *allreduce* has twice the runtime as *reduce-scatter*. There exist other ways of constructing *allreduce* such as reduce+broadcast in double binary tree [56]. However, we assert in §B.3 that other existing ways are suboptimal.

When performing reduce-scatter, it can be shown that whenever some node receives data from another node, it always results in less communication workload to immediately perform a reduction between the received data and its local

data with the resultant reduced data being sent out when required. Nodes c, d in figure 2 give such examples. Thus, we will implicitly assume this optimization.

2.1 Network model and communication schedules

The network topology is modeled as a directed graph, represented as the tuple $G = (V, E)$, where V denotes the set of nodes ($|V| = N$) and E denotes the set of directed edges. The optical network imposes a constraint that all nodes have degree d , which is the number of optical-link ports on each host and is ideally low and independent of N .

We use the well-known α - β cost model [34]. The cost of sending a message is assumed to consist of node latency α and a bandwidth runtime component, which is the inverse of the link bandwidth b , $\beta = \frac{1}{b}$. The cost of sending a message of size H between two nodes is given as $\alpha + \beta H$. This simple model has been shown to be a good proxy for characterizing communication costs on existing GPU interconnects [18, 43, 58]. The node bandwidth is denoted by B , with $B = db$.

Communication schedules can operate at a finer granularity than a shard. We define a chunk C to be a subset of the shard S . C is specified using an arbitrary *index set* identifying the elements of S contained within C . The schedule can be specified as which chunks are communicated over which links in any given *communication step* (or *comm step*). Thus, a schedule A for a topology G is a set of tuples $((w, C), (u, v), t)$ with $u, v, w \in V_G$, $(u, v) \in E_G$, and $t = 1, 2, \dots, t_{\max}$. $((w, C), (u, v), t)$ denotes that node u sends w 's chunk C to node v at step t , where w is the destination node in reduce-scatter. Note that a schedule can use different-sized chunks during its operation, and comm steps could differ in terms of data communicated.

A communication algorithm (G, A) uses the schedule A on topology G . The runtime of an algorithm can be broken down into a node latency component and a bandwidth component. The node latency component $T_L(A) = t_{\max}\alpha$ represents the cost of performing a collective operation on an infinitesimal amount of data. The bandwidth component is $T_B(A, M, B) = \sum_t T_B(A_t, M, B) = \sum_t \max_{(u,v) \in E_G} \frac{1}{B/d} \sum_{((w,C),(u,v)) \in A_t} |C|$, where M is the model size, B is the total egress bandwidth, and A_t is the subschedule at comm step t . We sometimes omit M and B to write $T_B(A)$. For d -regular graphs on N nodes, the lower bound on both the *reduce-scatter* and *all-gather* time is approximately $\alpha \log_d N + \frac{1}{B} \cdot \frac{M(N-1)}{N}$. The first term represents the node latency component associated with communicating across the diameter of a network, while the second term represents the transmission time across all links.

We analyze schedules in terms of **node latency optimality** and **bandwidth optimality**. We provide an informal description here and refer to Appendix B for details. We say an algorithm is *node latency optimal* if no algorithm with the same N, d can achieve lower T_L . In this paper, we often

use *Moore optimality* (def 11), which is a stricter but more well-defined form of *node latency optimality*. We define the schedule to be *bandwidth optimal* if the amount of data sent out by each node is $M \cdot \frac{N-1}{N}$ and the amount sent by each link is the same at any given step. The first condition ensures the minimum amount is sent, and the second implies balanced loads. We let T_B^* be the optimal bandwidth runtime $\frac{M}{B} \cdot \frac{N-1}{N}$.

The *ring allreduce* [37] algorithm (used by NCCL) incurs a runtime $t_{AR}^{\text{ring}} = 2\alpha(N-1) + \frac{2(N-1)M}{NB}$. Note that the node latency term is linear in N , while the bandwidth runtime is actually optimal. The *double binary trees* (DBT) algorithm [38], on the other hand, offers the advantage of logarithmic node latency but has suboptimal bandwidth.

2.2 Network Fabric

Our work identifies topologies and schedules helpful for a broad range of settings, such as *switchless physical circuits*, *patch-panel optical circuits*, and *optical circuit switches*. These options differ in cost, scalability, and reconfigurability [69].

Switchless physical circuits require the least amount of fabric hardware. However, the network topology must remain reasonably static for long periods, as the reconfiguration is manual. *Patch-panel optical circuits* provide a higher degree of reconfigurability by using a mechanical solution (e.g., robotic arms) to perform physical reconfigurations through a patch panel. The reconfigurations occur on the scale of tens of minutes, but the patch panel itself can scale to a large number of duplex ports and is reasonably cheap (e.g., 1008 ports at \$100 per port [62]). Both switchless physical circuits and patch-panel-based systems can benefit from a carefully curated static topology optimized for the workload.

Commercially available *optical circuit switches* (OCS) can perform reconfigurations in ≈ 10 ms, are more expensive than patch panels, and scale to fewer ports [19, 54] (e.g., Polatis 3D-MEMS switch has 384 ports at \$520 per port [54]). Though OCSes support faster reconfigurations, the delays are still too high to support the rewiring of the circuits during a typically-sized collective operation. Specifically, they cannot take advantage of algorithms designed for full-bisection switches, such as recursive halving/doubling [63, 71], that exploit high logical degree over time to provide both node latency and bandwidth optimality properties. Thus, OCSes can also benefit from the low-degree, reconfiguration-less connectivity provided by our synthesized topologies.

Research prototypes such as RotorNet[47] and Sirius[11] with μ s to ns reconfiguration latency, respectively, are based on demand-oblivious switch architectures designed to provide uniform bandwidth between all pairs of nodes in a round-robin fashion and 1-hop shortcuts. While recursive halving/doublings would benefit from fast reconfigurations, their traffic patterns are not uniform across all pairs of nodes,

nor can they tolerate the cost of indirect communications (Valiant Load Balance) that are bandwidth-inefficient (2x hit).

Finally, all of these technologies allow for a shared cluster to be split into multiple subclusters for running separate jobs, each configured with its own topology.

2.3 Related work

Classic HPC works on collectives investigated topologies such as ring, mesh, tori, hypercubes, de Bruijn, Kautz, etc. [13, 17, 20, 21, 29, 33, 36, 53]. However, these efforts optimize collectives for a given topology instead of determining an optimal topology for a specific collective and other design specifications, such as the number of nodes, node latency, and bandwidth. While bandwidth-efficient collectives are known for tori/meshes, and hypercubes [21], tori/meshes suffer from high latency (albeit lower than a ring), and hypercubes require a high degree which is unsuitable at large scale. Furthermore, these networks can be constructed only for specific values of N .

Topologies that have a near-optimal diameter for a given node degree d have also been proposed in HPC and data center networking. These include classic topologies such as de Bruijn and Kautz [29, 36], topologies with good “expansion” properties such as Jellyfish [60] and Xpander [66], and topologies that leverage high degree (100+) to realize large networks with a really low diameter (2 – 3), e.g., DragonFly [41], SlimFly [15], and variants [42, 74]. While single root broadcast and point-to-point collectives can be realized on such topologies [32], efficient scheduling of allreduce/reduce-scatter/allgather collectives, which are critical for ML training, has remained elusive.

ML training has driven researchers to optimize collective communications, in addition to orthogonal work on reducing parameter sizes [10, 22, 75]. Horovod [57], Baidu [30], and GLOO [52] implemented ring-based collectives. Recursive doubling, Bruck algorithm [63], and BlueConnect [25] optimize collectives on switch-based Clos-like topologies by following a bandwidth-optimal log-node-latency multi-phase *allreduce*, which isn’t appropriate for optical circuits.

Recent research has focused on generating good collective schedules for a given small-scale topology. In contrast, we consider *topology* also as a degree of freedom and jointly distill both the topology and the communication schedule for large-scale collective communications with thousands of nodes. The Blink library [68] uses a packing spanning trees approach to generate near bandwidth-optimal schedules but could include trees of $O(N)$ depth. Trees with $O(N)$ depth along with fine chunking required for packing spanning trees, invariably lead to higher node latency. The SCCL/M-SCCL library [18] uses a Satisfiability Modulo Theory (SMT) solver to find Pareto-optimal schedules in terms of both node

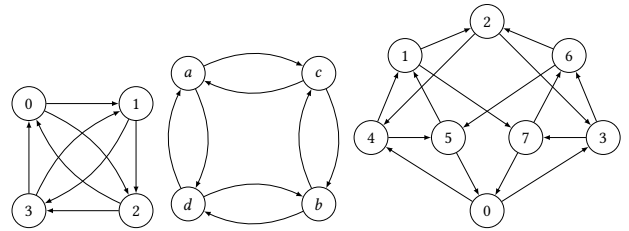


Figure 1: Example base graphs for $N = 4, d = 2$. directed circulant (left); complete bipartite $K_{2,2}$ (middle); synthesized diamond (right)

latency and bandwidth runtime, but it fails to generate efficient schedules in reasonable time beyond $N = 30$ nodes. While TACCL [58] improves the scalability of SCCL by using communication sketches as designer input to guide the collective synthesis process, it does not yield Pareto-optimal schedules and is still limited in scale, taking a prohibitive amount of time for $N > 100$. In contrast, our methods generate schedules for thousands of nodes in tens of seconds with provable performance guarantees for many graph families (e.g., distance-regular graphs, circulant graphs, etc.).

TopoOpt [69], the work closest to ours in spirit, jointly optimizes the network topology and the parallelization strategy in the context of hybrid data/model parallel ML training. It uses a collection of appropriately constructed rings to reduce the cost of model-parallel communications. We view our effort as complementary, given that we optimize data-parallel communications, especially since TopoOpt does not consider optimizing the topology or schedule for minimizing allreduce runtime. When data-parallel jobs dominate the workload, TopoOpt’s network topologies end up being various shifted rings, which have poor node latency performance, as we demonstrate in the evaluation.

3 Overview of our Approach

We seek to jointly identify high-performance network topologies and communication schedules for collectives. While it is feasible to construct topologies and schedules at a small scale, it is not obvious how to do so for larger cluster sizes or higher degrees. Consider, for instance, a cluster with $N=4, d=2$. As shown in Figure 1, some possible topologies are directed circulant graph, complete bipartite graph, and diamond digraph. One can construct schedules by hand that are both node latency and bandwidth optimal for reduce-scatter on these graphs. Figure 2 gives one such example for the complete bipartite graph. The schedule is node latency optimal because no one can finish reduce-scatter on 4 nodes in one comm step with degree 2. The schedule is bandwidth optimal because links are perfectly balanced, and no shard is sent twice. The question is how to scale topology and schedule generation to more nodes and comm steps?

Our approach, shown in Figure 3, identifies candidate topologies and schedules from a rich space of networks.

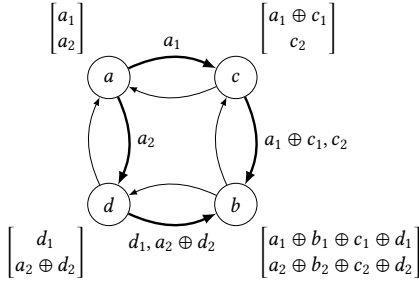


Figure 2: The reduce-scatter schedule of $K_{2,2}$. At each node i , the shard $S_b^{(i)}$ is divided into two halves i_1 and i_2 . Node a sends a_1 to c , and a_2 to d in the first comm step (for simplicity we denote $S_b^{(a_1)}$ by a_1). Nodes c, d reduce the received data to their local shards and send their reduced shards to b in the second comm step. Note that c sends to b the reduced data $a_1 \oplus c_1, c_2$ instead of a_1, c_1, c_2 to reduce the amount of communication on edge (c, b) , and the same happens for the send from d to b . After two steps, b has the reduced result $\bigoplus_{i \in \{a,b,c,d\}} S_b^{(i)}$. Applying the schedule w.r.t. a, c, d in parallel, we get the full *reduce-scatter* where each link transmits half a shard in the first step and a full shard in the second.

We construct **synthesized networks** by taking small base graphs and their associated base schedules and applying **expansion techniques** that not only assemble much larger topologies but also distill the associated schedules from the base schedules, while providing guarantees on node latency and bandwidth optimality (§4). The base graphs could be well-known structured topologies or other synthesized graphs with good network connectivity properties (§5). In addition to undirected topologies, our expansions also synthesize directed topologies as they can be realized in optical fabrics with the appropriate hardware support (simplex ports). **Generative networks** are well-known graphs that can be instantiated at various cluster sizes (e.g., Kautz graphs and de Bruijn graphs), but they require an additional algorithm for generating efficient schedules. We cast the **schedule generation** problem as a tractable optimization problem that balances load across links and minimizes node latency by making the data chunks stay on the shortest paths while respecting the dependency constraints of multi-hop aggregations (§6). Thus, we can assemble a large pool of networks and schedules, identify **Pareto-efficient** options from a node latency vs. bandwidth perspective, and select from them for a given workload using our **topology finder**. When two options are Pareto-efficient, it means one must be better than the other in either node latency or bandwidth performance but not in both. Finally, the **compiler** lowers the chosen topology and schedule to the runtime and hardware (§7).

4 Expansion Techniques

We present three techniques that can be iteratively applied to construct near-optimal collectives on arbitrarily large *synthesized networks* by starting from networks with a much smaller scale. The three techniques provide different options

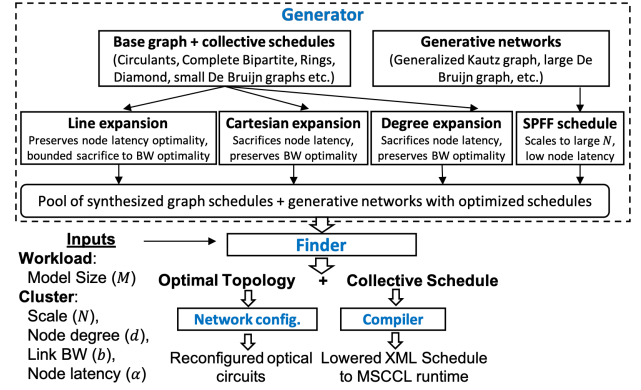


Figure 3: Schematic diagram of our approach

for increasing the size of the network and the per-node degree, while preserving the node latency or the bandwidth optimality properties of the base graph and schedule.

4.1 Line Graph Expansion

We borrow the following line graph transformation from graph theory, which transforms an input graph G into a larger graph $L(G)$ that contains a vertex for every edge in G .

DEFINITION 1 (LINE GRAPH). Given a directed graph (or digraph) G , each edge $(u, v) \in E_G$ corresponds to a vertex uv in the line graph $L(G)$. Vertex uu' is connected to vv' in digraph $L(G)$ if and only if $u' = v$.

Figure 4b gives an example of the line graph of the complete bipartite graph $K_{2,2}$ expressed as a digraph.

There are two key properties for a d -regular topology G :

- (1) $L(G)$ has the same degree as G , while $|V_{L(G)}| = d|V_G|$;
- (2) If and only if w_1, w_2, \dots, w_n is a (shortest) path in G , then $w_0 w_1, w_1 w_2, \dots, w_{n-1} w_n, w_n w_{n+1}$ is a (shortest) path from $w_0 w_1$ to $w_n w_{n+1}$ in $L(G)$ given $w_0 w_1 \neq w_n w_{n+1}$.

Property (1) enables us to expand a network topology to a larger size with the same degree, and Property (2) lets us map a schedule in G to a schedule in $L(G)$.

Given a schedule A_G for a topology G , we algorithmically construct the schedule $A_{L(G)}$ for $L(G)$. The schedule (formally described below) uses the path followed by the chunk (v, C) in G to construct the path for a corresponding chunk (vv', C) in $L(G)$. (The chunk (vv', C) is d times smaller since M is now sharded across a larger network.) The constructed path ends one hop before vv' , given that the graph's size has expanded, so the schedule includes an additional comm step to communicate the entire shard containing (vv', C) to the final destination vv' . Figure 4b illustrates the schedule construction with a sample path.

DEFINITION 2 (SCHEDULE OF LINE GRAPH). Given a *reduce-scatter* schedule A_G for topology G , let $A_{L(G)}$ be the schedule for line graph $L(G)$ containing:

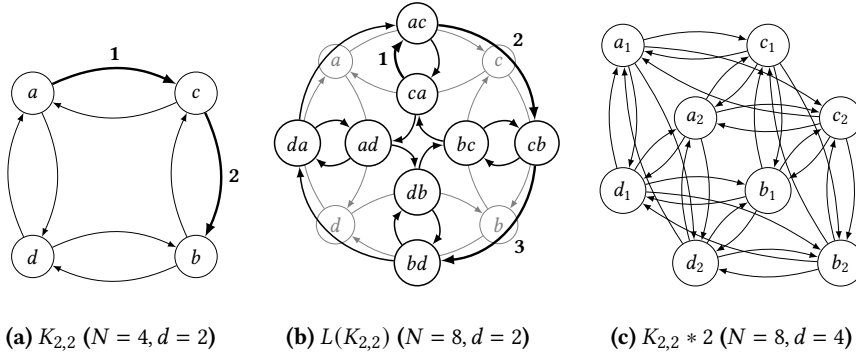


Figure 4: The complete bipartite topology $K_{2,2}$ with its line graph $L(K_{2,2})$ and degree expansion $K_{2,2} * 2$. In $L(K_{2,2})$, each vertex uv corresponds to the edge (u, v) in $K_{2,2}$. For any $uv, vw \in V_{L(K_{2,2})}$, there exists an edge from uv to vw . The figure shows an example of schedule transformation in line graph expansion. Suppose we want to know how to send from node ca to node bd in $L(K_{2,2})$. In $K_{2,2}$, node a sends a chunk C to c at $t = 1$, so node ca sends C to ac in $L(K_{2,2})$ by step 1 of definition 2: $((b, C), (a, c), 1) \Rightarrow ((bd, C), (ca, ac), 1)$. Node c sends C to b at $t = 2$, so similarly node ac sends C to cb : $((b, C), (c, b), 2) \Rightarrow ((bd, C), (ac, cb), 2)$. At $t = 3$ (assuming $t_{\max} = 2$), by step 2 of definition 2, cb will send the entire shard containing chunk C to bd and thus finish the communication: $((bd, S), (cb, bd), 3)$. One can also verify $ca \rightarrow ac \rightarrow cb \rightarrow bd$ being a shortest path.

1. $((vv', C), (wu, uu'), t)$ for all $((v, C), (u, u'), t) \in A_G$ and distinct $(v, v'), (w, u) \in E_G$;
2. $((vv', S), (uv, vv'), t_{\max} + 1)$ for all $(uv, vv') \in E_{L(G)}$ with $wu \neq vv'$. t_{\max} is the maximum comm step in A_G .

Corollary 2 in §A gives an equivalent construction for allgather. In practice, one can apply line graph expansion repeatedly to expand the reduce-scatter algorithm to an arbitrarily large scale. In terms of performance, Line graph expansion preserves Moore optimality and makes a bounded sacrifice to bandwidth optimality. Figure 5 shows how the performance evolves as we continuously apply line graph expansion to several base graphs. The node latency component increases due to the additional comm step introduced in the schedule, but this still preserves Moore optimality given the d -fold increase in topology size. The bandwidth performance deviates from optimality T_B^* but remains a constant factor away asymptotically. In fact, if the d -regular base graph has $\Omega(d^n)$ nodes, then T_B/T_B^* is at most $1 + O(1/d^{n+1})$ asymptotically. Thus, as in figure 5, the larger the size of the bandwidth-optimal base graph is, the closer the expanded algorithm is to bandwidth optimality. §D.1 gives a more formal and detailed analysis of line graph expansion.

4.2 Degree Expansion

While line graph expansion expands topology size, degree expansion expands topology degree. Given a d -regular topology G with no self-loops and its schedule A_G , degree expansion constructs an nd -regular topology $G * n$ by making n copies of each vertex in G and n^2 copies of each edge in G between corresponding pairs of vertices, i.e., $(u, v) \in E_G$ results in the introduction of all pairs $(u_i, v_j) \in E_{G^*}$ (see Figure 4c).

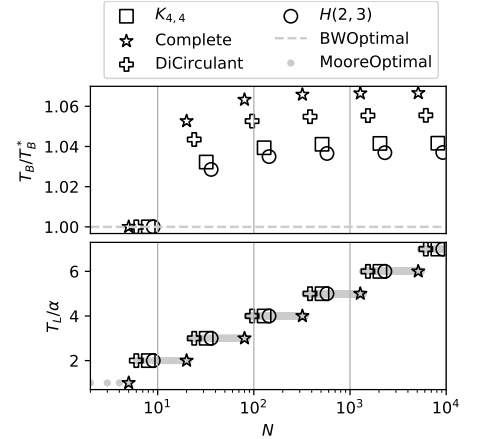


Figure 5: Line graph expansion on bandwidth and Moore optimal degree-4 base graphs: complete bipartite graph $K_{4,4}$, complete graph, directed circulant graph, and Hamming graph $H(2, 3)$. $T_B^* = \frac{M}{B} \cdot \frac{N-1}{N}$ is the optimal bandwidth runtime.

DEFINITION 3 (DEGREE EXPANDED TOPOLOGY). Given a topology G without self-loops and $n \in \mathbb{N}$, construct the degree expanded topology $G * n$ such that

1. For each vertex $v \in V_G$, add v_1, \dots, v_n to V_{G^*n} ,
2. For each edge $(u, v) \in E_G$, add (u_i, v_j) to E_{G^*n} for all i, j including $i = j$.

Based on the input schedule for G , we also construct a schedule A_{G^*n} that preserves bandwidth optimality while having only one additional comm step. Note first that for each chunk (w, C) in A_G , we now have n chunks (w_j, C) in A_{G^*n} . If a node u communicates (w, C) to node v in A_G , we construct a schedule wherein the chunks (w_j, C) are communicated by all u_i nodes to a particular v_j node; i.e., the traffic is split amongst the next hop choices based on the destination node. This provides the schedule for all node pairs except between the nodes that are copies of each other (e.g., c_1 and c_2 in Figure 6). We introduce an additional communication step at the beginning wherein each node u_i divides the shard that has to be sent to u_j into $n * d$ pieces and sends them to its immediate neighbors and then relies on the remainder of the schedule to communicate the data to the eventual destination. Figure 6 illustrates an application of the degree expanded schedule.

DEFINITION 4 (DEGREE EXPANDED SCHEDULE). Given a reduce-scatter schedule A_G for G , construct A_{G^*n} for $G * n$:

1. Divide shard S into equal-sized chunks C_1, \dots, C_{nd} . For each $u_i, u_j \in V_{G^*n}$ with $i \neq j$ and for each $(u_i, v_1), \dots, (u_i, v_{nd}) \in E_{G^*n}$, add $((u_j, C_\alpha), (u_i, v_\alpha), 1)$ to A_{G^*n} .
2. For all i, j including $i = j$ and for each $((w, C), (u, v), t)$ in A_G , add $((w_j, C), (u_i, v_j), t + 1)$ to A_{G^*n} .

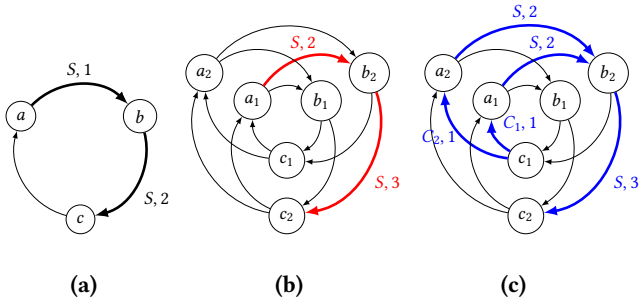


Figure 6: 3-node unidirectional ring and its degree expansion to $d = 2$. Figure (a) shows the path of transmission from a to c . Figure (b) shows the transformed path of transmission from a_1 to c_2 , and figure (c) shows the one from c_1 to c_2 . The texts next to edges denote the chunks and comm steps of the transmissions. In (a), the path from a to c is $((c, S), (a, b), 1), ((c, S), (b, c), 2)$. In (b), by step 2 of definition 3, there exists a path $((c_2, S), (a_1, b_2), 2), ((c_2, S), (b_2, c_2), 3)$ from a_1 to c_2 . As for (c), by step 1 of definition 3, c_1 will firstly send two equal-size chunks C_1 and C_2 to its two out-neighbors a_1 and a_2 respectively. Then, C_1 follows the path $((c_2, S), (a_1, b_2), 2), ((c_2, S), (b_2, c_2), 3)$ to c_2 , and C_2 follows the path $((c_2, S), (a_2, b_2), 2), ((c_2, S), (b_2, c_2), 3)$. Both paths are generated by step 2 of definition 3. Note that $C_1 \cup C_2 = S$.

Unlike line graph expansion, degree expansion preserves bandwidth optimality while introducing an additional comm step. However, degree expansion expands node degree along with the number of nodes. Unlike line graph expansion where the degree isn't changed, the additional comm step results in node latency sub-optimality since the diameter bound for higher-degree networks is smaller. A special case of degree expansion leverages the SPFF schedule from §6 and eliminates the additional comm step by Theorem 12 in §D.2.

4.3 Cartesian Product Expansion

From graph theory, the Cartesian product of two graphs G_1, G_2 is an expanded graph $G_1 \square G_2$ with size and degree equal to the product of G_1, G_2 's sizes and the sum of their degrees respectively.

DEFINITION 5 (CARTESIAN PRODUCT). *The Cartesian product digraph $G_1 \square G_2$ of digraphs G_1 and G_2 has vertex set $V_{G_1} \times V_{G_2}$ with vertex $\mathbf{u} = (u_1, u_2)$ connected to $\mathbf{v} = (v_1, v_2)$ iff either $(u_1, v_1) \in E_{G_1}$ and $u_2 = v_2$; or $u_1 = v_1$ and $(u_2, v_2) \in E_{G_2}$.*

This definition generalizes to a Cartesian product of more than two digraphs $G_1 \square G_2 \square \dots \square G_n$. When $G_1 = G_2 = \dots = G_n = G$, the product graph is denoted as the Cartesian power $G^{\square n}$. We use Cartesian Product and Cartesian Power in our topology and schedule expansion.

Cartesian Power Expansion Given a d -regular G and schedule A_G , we can construct a schedule $A_{G^{\square n}}$ for $G^{\square n}$, which is nd -regular and has $|V_G|^n$ nodes. Like degree expansion, Cartesian power expansion preserves bandwidth optimality and helps generate efficient topologies, including some well-known ones (see Appendix F). We describe how to construct allgather schedules for Cartesian power graphs by

using $\ell \times \ell$ torus (ℓ -ring^{□2}) as an example. Taking ℓ -ring allgather schedule A , a typical allgather schedule on $\ell \times \ell$ torus, as in hierarchical ring allreduce [65], is to perform schedule A along rings on one dimension first and then the other dimension. Consider two schedules: $A^{(1)}$ perform allgather on vertical rings first and then horizontal ones; $A^{(2)}$ perform allgather in the opposite order. $A^{(1)}, A^{(2)}$ use disjoint set of links at any comm step. Thus, we divide each shard in $\ell \times \ell$ torus into two halves and let them allgathered by $A^{(1)}, A^{(2)}$ separately. The combined schedule, where $A^{(1)}$ and $A^{(2)}$ are performed *simultaneously*, is bandwidth optimal. The node latency would be $2T_L(A)$.

The above schedule generalizes to arbitrary Cartesian power graphs (details in Appendix F). Appendix D.3 provides a formal definition of the schedule and an analysis of the bandwidth optimality of the Cartesian Power expansion.

Cartesian Product Expansion One can also construct a bandwidth optimal schedule for Cartesian product of distinct topologies (theorem 14 in §D.3) with T_L equal to the graph diameter. For example, one can generate bandwidth optimal schedule for $a \times b \times c$ 3D torus with unequal a, b, c . However, the schedule construction uses SPFF schedule generation, which we will introduce in §6.

5 Base Graphs and Generative Graphs

As mentioned earlier, the topologies we consider may be categorized into *synthesized* networks and *generative* networks. We describe here the base graphs used to derive synthesized networks, and the generative graphs used in combination with our SPFF schedule generation. Table 7 summarizes the important topologies and their main properties.

First, the base graphs for synthesized networks are small in size. They either come from well-known d -regular graphs in graph theory or custom-built ones by graph and schedule searches. These graphs have their own schedules and are the building blocks for our expansion techniques.

Well-known d -regular base graphs: Examples are rings, complete graphs, complete bipartite graphs, and the Hamming graphs. These graphs have simple structures given degree d and some other parameters. Thus, one can easily derive near-optimal (if not optimal) schedules for these graphs. SPFF schedule generation can give equally good schedules for these graphs as well.

Custom-built base graphs: We have also used discrete optimization techniques such as Mixed Integer Linear Program (MILP) (§H) and SMT solvers from SCCL [18] to generate base graphs and corresponding schedules. Because such techniques involve solving NP-hard problems, we can only do so at small scale. Examples are diamond graph (Figure 1, right) and modified de Bruijn graphs (§G). These graphs usually have even better performance, but they are limited in sizes ($d \leq 4, N \leq 20$).

Generative graphs Generative graphs are the larger and more complicated ones from graph theory. It is impractical to derive schedules for them manually or using discrete optimization. Thus, we invented SPFF linear program to generate schedules (§6). In addition, some of the graphs have special properties that allow us to mathematically prove performance guarantees. Specifically, we focus on the following three classes:

- Generalized Kautz Graph (§E.4): low- T_L graph that can be constructed for any N . Schedule generated by SPFF LP is at most one comm step away from Moore optimal.
- Distance Regular Graph (§E.5): graphs that can have large N while being bandwidth optimal and low in T_L .
- Circulant Graph (§E.7): bandwidth optimal graph that can be constructed for any N .

Generative networks are usually big enough for direct use in large-scale collective communication, but they can also be used as building blocks for expansion techniques. Generative networks that can be constructed for any N fill the gaps where expansion techniques cannot cover (e.g., prime N).

6 Shortest-Path-Farthest-First (SPFF) Schedule

We present a scalable schedule generation algorithm. By constraining the search space to a subspace (SPFF) of schedules, our algorithm formulates the scheduling problem as a linear program (LP), solvable in polynomial time unlike state-of-the-art approaches that involve NP-hard optimization (e.g., Blink [68], SCCL [18], and TACCL [58]). An SPFF schedule, although chosen from a constrained subspace, is shown to provide optimal schedules for a select class of topologies, and high-performance schedules for majority of topologies considered.

DEFINITION 6 (SHORTEST-PATH-FARTHEST-FIRST (SPFF) SCHEDULE). A reduce-scatter schedule A on G is an SPFF schedule if A satisfies: $((v, C), (u, w), t) \in A$ if and only if $d(u, v) = d(w, v) + 1 = D(G) + 1 - t$, where $D(G)$ is graph G 's diameter.

SPFF schedules must have the following properties: (i) Every chunk follows the shortest path from its source to destination (Shortest-Path); (ii) Every node sends out chunks in descending order of distances to their destinations (Farthest-First). The node latency of the SPFF schedule is $\alpha \cdot D(G)$, which is optimal for the topology.

In most topologies, there are multiple shortest paths from one vertex to another. To balance the load, we can divide shards into chunks to utilize multiple paths. Figure 7 shows an example. Node f wants to have the reduced shard of all nodes, and the shard is divided into three chunks. At comm step $t = D(G) + 1 - d(a, f) = D(G) - 2$, a sends all its chunks to b, c (two neighbors on a 's shortest paths to f). Since the distance between b, c and f is exactly $d(a, f) - 1$ (otherwise b, c are not on the shortest paths), b, c send out all their chunks

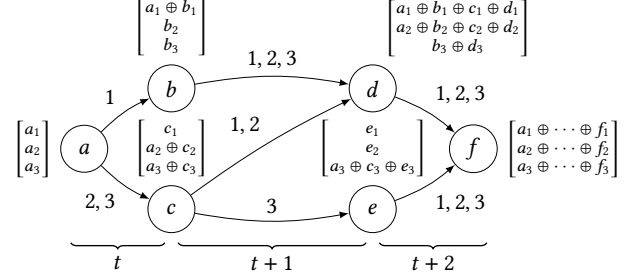


Figure 7: Example of SPFF reduce-scatter from node a to f on the same topology. Each node w has three chunks w_1, w_2, w_3 that need to be reduced at node f . The numbers on each link shows the indices of chunks being sent at the comm step. The vector near each node shows the memory state after reducing the received chunks. According to their distances to f , nodes $\{a\}, \{b, c\}, \{d, e\}$ send out chunks at comm step $t, t + 1, t + 2$ respectively, where $t = D(G) + 1 - d(a, f) = D(G) - 2$.

at the comm step immediately after. The same happens for d, e . In the end, f has the reduced shard of all nodes. Note that a, c can send chunks 1, 2, 3 arbitrarily to their neighbors, and one can easily check that the correctness of schedule is unaffected. In fact, in SPFF, a node only needs to ensure all chunks of the shard are sent to neighbors on the shortest paths at the correct comm step. *It does not matter which chunk is sent to which neighbor.* In practice, we only care about what percentage of the shard is sent to each neighbor. As long as the sum of percentages among all neighbors is one, the SPFF schedule is guaranteed to be correct.

Given a topology, there could be many SPFF schedules. We choose the SPFF schedule that minimizes bandwidth delay by formulating an optimization problem that controls the aforementioned percentages, in a manner that best distributes the communication load evenly across the network. Given comm step t , let $x_{u,w,v,t} \in [0, 1]$ be the percentage of shard sent through link (u, w) with destination v . For instance, in the left example of Figure 7, we have $x_{a,b,f,t} = 1/3$ and $x_{c,d,f,t+1} = 2/3$. Note that $x_{u,w,v,t}$ is defined if and only if $(u, w) \in E_G$ and $d(u, v) = d(w, v) + 1 = D(G) + 1 - t$ (i.e. w is a neighbor of u on u 's shortest paths to v). Given u and t , we have LP:

$$\begin{aligned}
 & \text{minimize} && U_{u,t} \\
 & \text{subject to} && \sum_w x_{u,w,v,t} \leq U_{u,t}, \quad \forall (u, w) \in E_G \\
 & && \sum_w x_{u,w,v,t} = 1, \quad \forall v \in N_{D(G)+1-t}(u) \\
 & && 0 \leq x_{u,w,v,t} \leq 1, \quad \forall w, v
 \end{aligned} \tag{1}$$

$N_{D(G)+1-t}(u)$ denotes the set of nodes $D(G) + 1 - t$ away from u . To compute a reduce-scatter SPFF schedule for topology G , one needs to solve an independent LP (1) for each comm step $t \in \{1, \dots, D(G)\}$ and vertex $u \in V_G$. One can speedup this process by solving LPs in parallel. The overall bandwidth

runtime is given by

$$T_B = \frac{M/N}{B/d} \sum_{t=1}^{D(G)} \max_{u \in V_G} U_{u,t}. \quad (2)$$

Given a topology G , any SPFF schedule gives the same T_L . Since LP (1) gives a schedule with minimum T_B , it gives the optimal schedule in SPFF schedule space. The latter is not necessarily the optimal schedule among all possible schedules. However, as we prove in §E, it is globally optimal in some cases like circulant graphs and distance-regular graphs.

The LP is used to generate schedules for various topologies, e.g., generalized Kautz graph, circulant graphs, and some cartesian/degree expanded topologies. The LP can also be used to generate chunked schedules (§E.1) and schedules for heterogeneous networks (§E.2).

7 Topology Search & Schedule Compilation

We implement a general tool for producing high-performance topologies and collective communication schedules for arbitrary scale N and degree d . As shown in Figure 3, the tool comprises of three main components: a generator, a finder, and a compiler. The implementation serves to validate our models and evaluate the performance of our schedules in practice (§8.1).

Generator The generator maintains a library of all the base graphs and generative graphs defined in §5, along with the expansion algorithms for expanding topologies and schedules (§4), and the SPFF schedule generation LP (§6). The library also defines an optimal schedule for many of the base graphs where such a schedule is straightforward to define (e.g., ring, complete, complete bipartite, hamming).

Finder The finder determines the Pareto-efficient topologies for a given N and d . It starts with the different base graphs and their schedules at small sizes and degrees and iteratively applies different expansion techniques to reach the target scale N and degree d . We use mathematical results (§D) for deriving the performance of topologies in terms of node latency and bandwidth runtime. The finder also generates bidirectional topologies from unidirectional ones using the technique in §K. For all topologies, the modeled reduce-scatter (similarly allgather) runtime is of the form $\alpha x + (M/B)y$. The search finds all the Pareto-efficient topologies for a given N and d , regardless of the actual values of α, M, B . The list is then filtered to determine the best performing topologies for the specific testbed and workload parameters α, B and message size distribution of M .

Table 2 illustrates this process for $N = 1024$ and $d = 4$. The generalized Kautz graph $\Pi_{4,1024}$ (§E.4) is Moore optimal and the Cartesian power of the Cartesian product of two unidirectional rings $(\text{UniRing}(1, 4) \square \text{UniRing}(1, 8))^{\square 2}$ is bandwidth

Topology	x	y	$2\alpha x + 2\frac{M}{B}y$
$\Pi_{4,1024}$	5	1.332	323.5us
$L^3(C(16, \{3, 4\}))$	6	1.020	291.0us
$L^2(\text{Diamond}^{\square 2})$	8	1.004	328.4us
$L(\text{DBJMod}(2, 4)^{\square 2})$	11	1.000	387.8us
$(\text{UniRing}(1, 4) \square \text{UniRing}(1, 8))^{\square 2}$	20	0.999	567.6us
Theoretical Lower Bound	5	0.999	267.6us

Table 2: Pareto-efficient topologies at $N = 1024, d = 4$. Last column shows allreduce runtime for $\alpha = 10\mu\text{s}$ and $M/B = 1\text{MB}/100\text{Gbps}$. The x and y are reduce-scatter/allgather values, which are half of those of allreduce. In comparison, Shifted Ring and DBT take 20640us and 1800us respectively.

optimal, where $\text{UniRing}(d, N)$ is a unidirectional ring of degree d and size N . The other Pareto-efficient topologies are line graph expansions of circulant graph $C(16, \{3, 4\})$ (§E.7), Diamond graph (§H, Figure 1 right), and modified de Bruijn $\text{DBJMod}(2, 4)$ (§G). The table also shows the allreduce runtime. $L^3(C(16, \{3, 4\}))$ has the best performance, within 10% of the theoretical lower bound.

Our current implementation exhaustively explores the base graphs and expansions and runs under a minute for all $d = 2, 4, 8, 16$ and N up to 2000. While this can be sped up, we find it acceptable for now given that the search is performed once for a given N and d , and candidates can be cached for future use.

Compiler The compiler lowers the collective algorithm to an XML schedule that can be executed by the MSCCL runtime [48]. MSCCL is an open source collective communications library that extends NCCL [3] with an interpreter providing the ability to program custom collectives. Collective schedules are defined in XML as instructions (send/receive/reduce/copy) within GPU threadblocks. The XML interface offers granular control over scheduling, such as the number of threadblocks and channels, instruction dependencies and fusion.

We found that schedules produced by MSCCL’s compiler [26, 49] performed poorly on our direct-connect testbed. Micro-benchmarking on our testbed showed that the send/receive instructions are the main source of node latency, and it is significantly faster to issue a grouped send/receive instruction for multiple chunks than to issue multiple send/receive instructions per chunk. We implemented our own compiler that copies non-contiguous chunks into contiguous chunks in a scratch buffer and sends/receives them in a single instruction. We used the compiler to generate more than 1K schedules for different topologies and algorithms and verify their correctness and performance against our models.

8 Evaluation

We present performance evaluation results on a 12-node direct-connect optical testbed along with analytical and simulation results at large scales. All schedules in this paper are model checked with definitions in §A. We conducted experiments to validate the $\alpha - \beta$ cost model on our testbed

(§J). Even at the scale of our testbed ($N \leq 12$), our topologies and schedules are shown to outperform baselines (e.g., ring-based collectives, DBT), and analytical models for large-scale settings show benefits as high as 10x over the best-performing baseline (§8.3). DNN training experiments on the testbed show our distilled topologies and schedules improve upon baselines by more than 30% on average (§8.4). In large-scale simulations of DNN training ($N = 1024$), our topology-schedule solutions beat best-performing baselines by a factor of 25x in allreduce time and 6x in minibatch training time (§8.4). Our schedules are matched to the underlying direct-connect physical topology and can fully exploit the link bandwidth, unlike popular widely adopted algorithms such as NCCL and recursive halving/doubling (§8.5). Finally, our schedule generation approach is more scalable and is orders of magnitude faster than state-of-the-art efficient schedule generators, such as SCCL and TACCL (§8.6).

8.1 Direct-connect optical testbed

Our testbed consists of 12 servers, each with an NVIDIA A100 GPU [7] and a 100 Gbps HP NIC [8], configured as 4x25Gbps breakout interfaces [6]. The NICs are directly connected via a Telescent optical patch panel [9]. Our testbed can realize topologies by reconfiguring the patch panel. We limit our evaluation to bidirectional topologies. While unidirectional topologies can be realized by configuring the patch panel in simplex mode, the requisite overlay routing for the reverse path traffic (acks etc.) is currently only supported using routing rules performed by the host kernel as opposed to the NIC, leading to unpredictable RTTs. Therefore, we can functionally validate unidirectional topologies on our testbed, but we cannot accurately evaluate their performance. Note that newer NICs [1, 4, 5] do support hardware offloading for these rules, and we will examine them in the future.

8.2 Experiment Setup

We evaluate allreduce performance on various model sizes on topologies of sizes $N \in [5, 12]$, $d = 4$ on our testbed; The best topologies are in Table 3. We evaluate the impact on end-to-end DNN training on $N = 8$, $d = 4$ topology on the testbed in §8.4; We also analyze larger topologies using simulations.

Baselines: We evaluate against the following topology-schedule baselines with $d = 4$: (1) *ShiftedRing* from TopoOpt [69], which improves upon NCCL ring [3]. It is the topology used by TopoOpt for data-parallel training. The topology is a superposition of two bidirectional rings, each all-reducing half of the data. (2) *ShiftedSPFFRing* uses *ShiftedRing* topology and augments it with our SPFF schedule on each ring (§E.3) to reduce node latency. (3) Double Binary Trees, also implemented in NCCL, uses the topology and schedule from [38, 56].

Methodology: We use the MSCCL runtime [18, 26, 48] to evaluate the generated schedules for our topologies. We sweep through several key schedule parameters, such as the protocol (Simple or LL), number of channels (1, 2, 4, or 8), different degrees of pipelining for DBT baseline, etc., and choose the best-performing schedule for each message size. For DNN training, we pass our schedules to PyTorch with the MSCCL backend.

8.3 AllReduce Collective Performance

Figure 8 shows experimental results for varying topology sizes N and model sizes M , and Table 3 shows our best-performing topology from Pareto-efficient options at each scale. We observe that in the small message regime ($M = 1KB$), our solution beats shifted ring by a significant margin (at $N = 12$, $\sim 60\%$ and $\sim 75\%$ lower than ShiftedSPFFRing and ShiftedRing respectively) and also outperforms DBT ($\sim 20\%$ at $N = 8, 10, 12$). Note that at small model sizes, the runtime is dominated by node latency T_L , and hence we can significantly outperform shifted ring.

In the large message regime ($M = 1GB$), our solution beats DBT by a significant margin ($\sim 50\%$ lower at $N = 8, 10, 12$) and matches the performance of shifted ring. At large model sizes, the runtime is dominated by bandwidth runtime T_B , and since the shifted ring is BW optimal, we can only match its performance. Due to the influence of both node latency and BW runtime at intermediate message sizes ($M = 1MB$), our solution outperforms both shifted ring (at $N = 12$, $\sim 50\%$ and $\sim 25\%$ lower than ShiftedRing and ShiftedSPFFRing respectively) and DBT ($\sim 45\%$ at $N = 8, 10, 12$) in this regime. Note that although right now our gains over shifted ring baselines diminish as M increases, future increases in hardware bandwidth will enhance gains at large M .

Figure 9 shows the runtime comparison for large N based on our analytical model. Our solutions perform orders of magnitude faster ($\sim 50x$ at $N = 2000$) than the shifted ring baselines due to the latter’s linear growth in node latency with increasing N . Although DBT’s node latency is logarithmic in N , its poor bandwidth utilization leads to significantly higher total runtime ($\sim 10x$ at $N = 2000$). Note that our approach yields high-performing solutions for a wide range of N s and degrees; see §I for details on Pareto-efficient topologies.

In summary, the results demonstrate that (1) *efficient schedules (SPFF) when applied to a topology (here, ShiftedRing) yield benefits that generally increase with scale*; (2) *further optimizing the topology leads to more benefits*; and (3) *the best topology depends on scale validating the need for cluster- and workload-aware topology search*.

N	Topology	T_L
5	Complete Graph: K_5	2α
6	Degree Expansion of Complete graph: $K_3 * 2$	4α
7	Circulant Graph: $C(7, \{2, 3\})$	4α
8	Complete Bipartite Graph: $K_{4,4}$	4α
9	Hamming Graph: $H(2, 3)$	4α
10	Degree Expansion of SPFF Bidirectional Ring: BiRing(2, 5) * 2	4α
11	Circulant Graph: $C(11, \{2, 3\})$	4α
12	Circulant Graph: $C(12, \{2, 3\})$	4α

Table 3: Our Best Topologies at $d = 4$. All topologies listed above are bandwidth optimal, i.e., $T_B = 2 \frac{M}{B} \cdot \frac{N-1}{N}$.

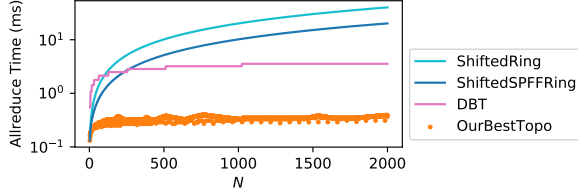


Figure 9: Comparison against naive ring, ring with SPFF schedule, and double binary tree at different N for $d = 4$, $\alpha = 10\mu s$, and $M/B = 1MB/100Gbps$.

8.4 DNN Training Performance

Figure 10a shows the improvements in total allreduce time and per-minibatch time across all layers on several common DNN models. Our solution improves total allreduce time by 30% and 50% (minibatch time by 10% and 25%) on average against ShiftedRing and DBT, respectively; ShiftedSPFFRing outperforms ShiftedRing in every model due to its improvement in node latency. Since optimizations such as wait-free backpropagation [76] overlap computation and communication, some improvements in collective communication are hidden by the computation within the minibatch time.

The gains depend on layer sizes in each model. For models with many large layers (e.g., vgg16 [59]) bandwidth optimal topologies like $K_{4,4}$ and shifted rings are better; For models with mostly smaller layers (e.g., squeezenet1_1 [35]), topologies with low node latencies like $K_{4,4}$, double binary tree, and ShiftedSPFFRing perform better. Since our chosen $K_{4,4}$ topology is both bandwidth and node latency optimal, it delivers the best performance across all models.

Large-Scale Simulation We then *simulate* DNN training at a much larger scale ($N = 1024$) than our testbed permits. We gather the *ready time* of each layer and simulate wait-free backpropagation [76]. Suppose layers have been sorted in ascending order of their ready times. Let r_i and M_i be the ready time and size of layer i , respectively. The finish time f_i for layer i is then calculated as $f_i = \max(f_{i-1}, r_i) + 2 [T_B(A_G, M_i, B) + T_L(A_G)]$. The rationale behind this is that the allreduce of layer i starts only if (1) layer $i-1$ has finished allreduce, and (2) layer i has been ready for allreduce. Thus, the finish time of the last layer f_{\max} is the backpropagation

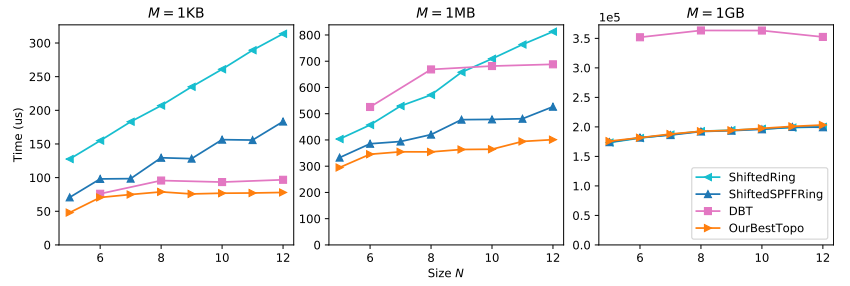


Figure 8: Comparison of allreduce runtimes on our testbed at $M = 1KB, 1MB$, and $1GB$. The topologies we used for “OurBestTopo” are listed in Table 3.

time. We run simulations on various DNNs and compare the best of our Pareto-efficient topologies (table 2) against the ShiftedRing and DBT. The results are shown in Figure 10b. Across the eleven DNN workloads, our best topology has on average 73x and 25x lower allreduce time (13x and 6x lower minibatch training time) than ShiftedRing and DBT, respectively, while being only 6.7% on average (at most 11.6%) above the theoretical lower bound of allreduce time and $< 0.1\%$ above the lower bound of minibatch time.

In summary, *allreduce speedups directly translate to speedups in DNN training, increasing with scale*. Specifically, benefits from node latency optimization have a large impact at scale.

8.5 Popular Algorithms applied to Direct-Connect

Next, we assess the performance of today’s state-of-the-art allreduce algorithms over two popular direct-connect topologies. Baseline algorithms, mainly NCCL Ring and recursive halving & doubling (RH&D), are heavily used by the AI/ML and HPC communities and were originally designed for packet-switched fabrics. We choose hypercube as the baseline topology because it is widely used in collective communication, and the communication pattern of RH&D perfectly matches the connections of the hypercube. We also try the twisted hypercube [28] baseline, a variant of hypercube that has a lower diameter.

Figure 11 compares the baselines against our SPFF schedule when run over either hypercube or twisted hypercube with $N = 8, d = 3$ on the testbed. At small M , all schedules and topologies perform roughly the same, except SPFF can take advantage of the lower diameter of twisted hypercube and achieve $\sim 20\%$ lower runtime. At large M , because SPFF can achieve bandwidth optimality on both topologies, it performs even better with 60%+ lower runtime. RH&D and NCCL perform poorly as M grows because they cannot utilize all $d = 3$ links simultaneously. At every step in the RH&D schedule, a node only communicates with one other node over a single link, utilizing at most a third of the total bandwidth (similarly with NCCL). Also, because of the schedule not being matched to the topology, some pairs of

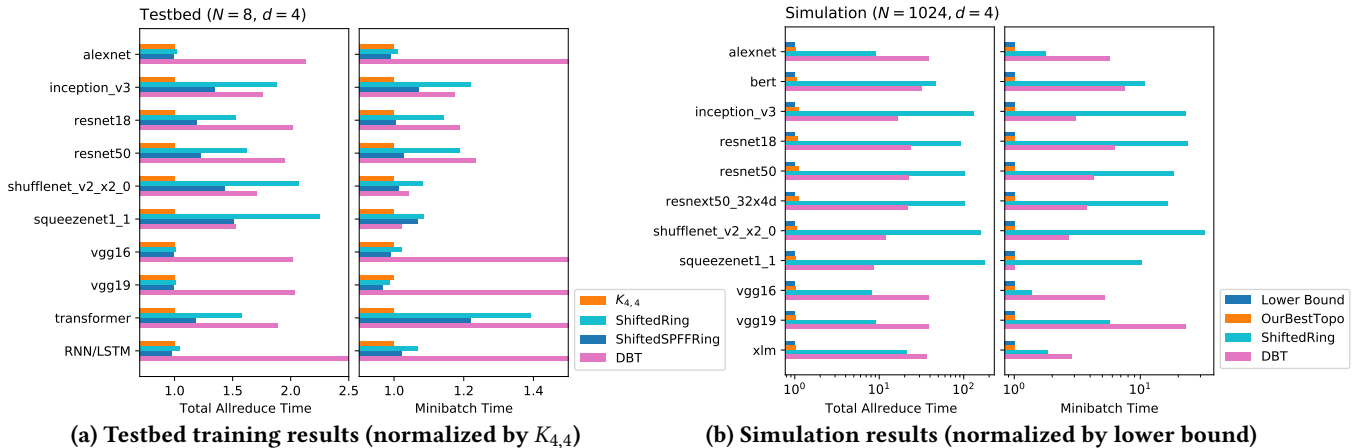


Figure 10: Comparison with baseline topologies in DNN training. The left figure shows results from actual training on our testbed of 8 Nvidia A100 GPUs. All models are using batch size 64. The total allreduce time is the sum of allreduce time of all layers in the model. The right figure shows the simulation results with $N = 1024$, $\alpha = 10\mu\text{s}$, $B = 100\text{Gbps}$ and $d = 4$. The ready times of layers were gathered from running on Nvidia Tesla V100-SXM2-16GB.

nodes have to occupy multiple hops of links to communicate, increasing congestion as M increases.

In summary, *unlike today’s popular allreduce algorithms, our schedules can fully exploit direct-connect fabrics.*

8.6 Scalability Comparison

In the context of techniques that generate efficient schedules, SCCL [18] and TACCL [58] are the closest in spirit to SPFF. Note that the expansion of base graph schedules is much faster than SPFF due to direct mathematical construction; therefore, we restrict this study to SPFF. Figure 12 shows the runtime comparison between SCCL and SPFF when generating reduce-scatter schedules for hypercube, 2D torus, and degree-2 de Bruijn graphs. SCCL, which uses an SMT solver, fails to generate a schedule in reasonable time beyond $N = 30$. In comparison, SPFF linear program is faster by orders of magnitude while generating schedules with similar performance (detailed result in Appendix as Figure 20). SPFF’s novelty lies in representing the amount of data as a continuous value ($x \in [0, 1]$) instead of a discrete number of chunks, thereby relaxing the integer linear program to an LP that can be decomposed and solved for each node and step (§6). On the other hand, SCCL solves an NP-hard combinatorial search over discrete chunks and rounds and steps and has to iterate through unsat formulations. Although SPFF cannot generate all Pareto-optimal schedules, SCCL can only do so for small N and cannot generate any schedule for larger N .

While TACCL improves the scalability of SCCL, it formulates the scheduling problem as a mixed integer linear program (MILP), which is also NP-hard problem. As a result, TACCL is still limited in scale – their technique was reported to take 41s to synthesize an allgather schedule for $N = 32$, 8 minutes for $N = 80$, and 11 hours for $N = 128$.

In summary, *our schedule generation algorithms are highly scalable generating high-quality schedules for thousands of nodes in tens of seconds.*

9 Concluding Remarks

Collective communications are critical to both large-scale ML training and HPC. Current network architectures do not exploit the regular patterns of distributed data flow embedded in these collectives and often suffer from high node latency or bandwidth contention. In this paper, we demonstrated a novel direct-connect network design of jointly optimizing topology and schedule by exploiting the concurrent aggregation and distribution-oriented data flow patterns. By leveraging scalable graph-theoretic approaches, our algorithm framework can provide maximally performant and resource-efficient topologies and schedules even for large scales. This paper raises no ethical issues.

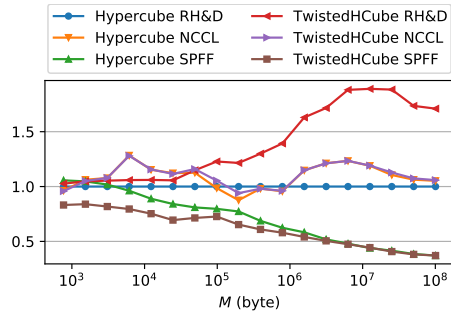


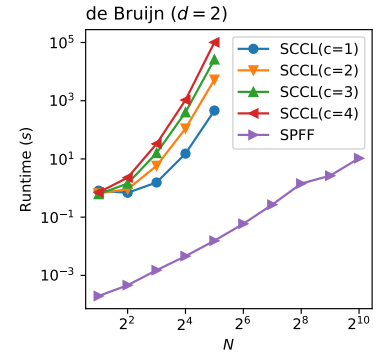
Figure 11: Comparing switch-based allreduce (recursive halving & doubling (RH&D), NCCL) against SPFF schedule on hypercube and twisted hypercube. The runtimes are normalized by the runtime of recursive halving & doubling on hypercube.

References

- [1] ConnectX-6 Dx Datasheet. <https://www.nvidia.com/content/dam/en-zz/Solutions/networking/ethernet-adapters/connectX-6-dx-datasheet.pdf>.
- [2] DistanceRegular.org. <https://www.distanceregular.org>.
- [3] NCCL. <https://github.com/NVIDIA/nccl>.
- [4] P2200G - 2 x 200GbE PCIe NIC. <https://www.broadcom.com/products/ethernet-connectivity/network-adapters/200gb-nic-ocp/p2200g>.
- [5] RockPort NC1225 network card. <https://rockportnetworks.com/product/>.
- [6] AOI 100G PSM4 Transceiver, 2020. <https://www.ebay.com/itm/234092018446?hash=item3680f8bb0e:g:WoMAAOSwLFJg8dKF>.
- [7] NVIDIA A100 Tensor Core GPU, 2021. <https://www.nvidia.com/en-us/data-center/a100/>.
- [8] HPE Ethernet 4x25Gb 1-port 620QSFP28 Adapter, 2022. https://support.hpe.com/hpsc/public/docDisplay?docId=emr_na-c05220334.
- [9] Telescent G4 Network Topology Manager, 2022. <https://www.telescent.com/products>.
- [10] ALISTARH, D., GRUBIC, D., LI, J. Z., TOMIOKA, R., AND VOJNOVIC, M. Qsgd: Communication-efficient sgd via gradient quantization and encoding. In *Proceedings of the 31st International Conference on Neural Information Processing Systems (Red Hook, NY, USA, 2017)*, NIPS'17, Curran Associates Inc., p. 1707–1718.
- [11] BALLANI, H., COSTA, P., BEHRENDT, R., CLETHEROE, D., HALLER, I., JOZWIK, K., KARINOU, F., LANGE, S., SHI, K., THOMSEN, B., AND WILLIAMS, H. Sirius: A flat datacenter network with nanosecond optical switching. In *Proceedings of the Annual Conference of the ACM Special Interest Group on Data Communication on the Applications, Technologies, Architectures, and Protocols for Computer Communication (New York, NY, USA, 2020)*, SIGCOMM '20, Association for Computing Machinery, p. 782–797.
- [12] BANG, S., DUBICKAS, A., KOOLEN, J., AND MOULTON, V. There are only finitely many distance-regular graphs of fixed valency greater than two. *Advances in Mathematics* 269 (2015), 1–55.
- [13] BARNETT, M., SHULER, L., VAN DE GEIJN, R., GUPTA, S., PAYNE, D. G., AND WATTS, J. Interprocessor collective communication library (intercom). In *Proceedings of IEEE Scalable High Performance Computing Conference (1994)*, IEEE, pp. 357–364.
- [14] BERMOND, J.-C., HOMOBONO, N., AND PEYRAT, C. Connectivity of kautz networks. *Discrete Math.* 114, 1-3 (apr 1993), 51–62.
- [15] BESTA, M., AND HOEFLER, T. Slim fly: A cost effective low-diameter network topology. In *Proceedings of the International Conference for High Performance Computing, Networking, Storage and Analysis (2014)*,

N	SCCL				SPFF
	c = 1	c = 2	c = 3	c = 4	
Hypercube					
4	0.59	0.64	0.68	0.72	< 0.01
8	0.86	1.22	1.86	2.48	< 0.01
16	21.4	48.4	130	573	< 0.01
32	> 10 ⁴	> 10 ⁴	> 10 ⁴	> 10 ⁴	0.03
1024	> 10 ⁴	> 10 ⁴	> 10 ⁴	> 10 ⁴	52.7
2D Torus (n × n)					
4	0.61	0.63	0.67	0.76	< 0.01
9	1.00	1.51	2.22	3.44	< 0.01
16	17.5	60	131	603	< 0.01
25	3286	5641	> 10 ⁴	> 10 ⁴	0.01
36	> 10 ⁴	> 10 ⁴	> 10 ⁴	> 10 ⁴	0.03
2500	> 10 ⁴	> 10 ⁴	> 10 ⁴	> 10 ⁴	61.1

Figure 12: Comparing schedule generation runtimes (in seconds) of SCCL and SPFF. Both were run to generate reduce-scatter schedules for different topologies. The setup of SCCL is to generate schedules with least number of comm steps and with chunks=1,2,3,4 (number of chunks per shard).



- SC '14, IEEE Press, p. 348–359.
- [16] BOESCH, F., AND WANG, J.-F. Reliable circulant networks with minimum transmission delay. *IEEE Transactions on Circuits and Systems* 32, 12 (1985), 1286–1291.
- [17] BOKHARI, S. H., AND BERRYMAN, H. Complete exchange on a circuit switched mesh. In *Proceedings Scalable High Performance Computing Conference SHPCC-92*. (1992), IEEE, pp. 300–306.
- [18] CAI, Z., LIU, Z., MALEKI, S., MUSUVATHI, M., MYTKOWICZ, T., NELSON, J., AND SAARIKIVI, O. *Synthesizing Optimal Collective Algorithms*. Association for Computing Machinery, New York, NY, USA, 2021, p. 62?75.
- [19] Calient Optical Circuit Switch. <https://www.calient.net/products/edge640-opticalcircuit-switch/>.
- [20] CHAN, E., HEIMLICH, M., PURKAYASTHA, A., AND VAN DE GEIJN, R. Collective communication: Theory, practice, and experience: Research articles. *Concurr. Comput. : Pract. Exper.* 19, 13 (sep 2007), 1749–1783.
- [21] CHAN, E., VAN DE GEIJN, R., GROPP, W., AND THAKUR, R. Collective communication on architectures that support simultaneous communication over multiple links. In *Proceedings of the eleventh ACM SIGPLAN symposium on Principles and practice of parallel programming (2006)*, pp. 2–11.
- [22] CHEN, C.-Y., CHOI, J., BRAND, D., AGRAWAL, A., ZHANG, W., AND GOPALAKRISHNAN, K. Adacom: Adaptive residual gradient compression for data-parallel distributed training. In *Proceedings of the Thirty-Second AAAI Conference on Artificial Intelligence and Thirtieth Innovative Applications of Artificial Intelligence Conference and Eighth AAAI Symposium on Educational Advances in Artificial Intelligence (2018)*, AAAI'18/IAAI'18/EAAI'18, AAAI Press.
- [23] CHENG, Q., BAHADORI, M., GLICK, M., RUMLEY, S., AND BERGMAN, K. Recent advances in optical technologies for data centers: a review. *Optica* 5, 11 (2018), 1354–1370.
- [24] CHENG, Q., RUMLEY, S., BAHADORI, M., AND BERGMAN, K. Photonic switching in high performance datacenters. *Optics express* 26, 12 (2018), 16022–16043.
- [25] CHO, M., FINKLER, U., AND KUNG, D. Blueconnect: Novel hierarchical all-reduce on multi-tired network for deep learning. In *Proceedings of the 2nd SysML Conference (2019)*.
- [26] COWAN, M., MALEKI, S., MUSUVATHI, M., SAARIKIVI, O., AND XIONG, Y. Gc3: An optimizing compiler for gpu collective communication. arXiv preprint, February 2022.
- [27] DAHLHAUS, E., AND KARPINSKI, M. Parallel construction of perfect matchings and hamiltonian cycles on dense graphs. *Theoretical computer science* 61, 2-3 (1988), 121–136.
- [28] ESFAHANIAN, A.-H., NI, L., AND SAGAN, B. The twisted n-cube with application to multiprocessing. *IEEE Transactions on Computers* 40, 1

- (1991), 88–93.
- [29] FAIZIAN, P., MOLLAH, M. A., YUAN, X., ALZAI, Z., PAKIN, S., AND LANG, M. Random regular graph and generalized de bruijn graph with k -shortest path routing. *IEEE Transactions on Parallel and Distributed Systems* 29, 1 (2017), 144–155.
- [30] GIBIANSKY, A. Bringing hpc techniques to deep learning. *Baidu Research, Tech. Rep.* (2017).
- [31] GODSIL, C., AND ROYLE, G. F. *Algebraic graph theory*, vol. 207. Springer Science & Business Media, 2001.
- [32] HEYDEMANN, M.-C., OPATRYN, J., AND SOTTEAU, D. Broadcasting and spanning trees in de bruijn and kautz networks. *Discrete applied mathematics* 37 (1992), 297–317.
- [33] HO, C.-T., AND JOHNSON, S. L. Distributed routing algorithms for broadcasting and personalized communication in hypercubes. In *ICPP* (1986), pp. 640–648.
- [34] HOCKNEY, R. W. The communication challenge for mpp: Intel paragon and meiko cs-2. *Parallel computing* 20, 3 (1994), 389–398.
- [35] LANDOLA, F. N., HAN, S., MOSKIEWICZ, M. W., ASHRAF, K., DALLY, W. J., AND KEUTZER, K. Squeezenet: Alexnet-level accuracy with 50x fewer parameters and <0.5mb model size, 2016.
- [36] IMASE, AND ITOH. A design for directed graphs with minimum diameter. *IEEE Transactions on Computers C-32*, 8 (1983), 782–784.
- [37] JEAUGEY, S. Optimized inter-gpu collective operations with nccl 2. <https://developer.nvidia.com/nccl>, 2017.
- [38] JEAUGEY, S. Massively scale your deep learning training with nccl 2.4. <https://developer.nvidia.com/blog/massively-scale-deep-learning-training-nccl-2-4/>, 2019.
- [39] KEWITSCH, A. S. Large scale, all-fiber optical cross-connect switches for automated patch-panels. *J. Lightwave Technol.* 27, 15 (Aug 2009).
- [40] KHANI, M., GHOBADI, M., ALIZADEH, M., ZHU, Z., GLICK, M., BERGMAN, K., VAHDAT, A., KLENK, B., AND EBRAHIMI, E. Sip-ml: High-bandwidth optical network interconnects for machine learning training. In *Proceedings of the 2021 ACM SIGCOMM 2021 Conference* (New York, NY, USA, 2021), SIGCOMM '21, Association for Computing Machinery, p. 657–675.
- [41] KIM, J., DALLY, W. J., SCOTT, S., AND ABTS, D. Technology-driven, highly-scalable dragonfly topology. In *2008 International Symposium on Computer Architecture* (2008), pp. 77–88.
- [42] LAKHOTIA, K., BESTA, M., MONROE, L., ISHAM, K., IFF, P., HOEFLER, T., AND PETRINI, F. Polarfly: A cost-effective and flexible low-diameter topology. In *Proceedings of the International Conference on High Performance Computing, Networking, Storage and Analysis* (2022), SC '22, IEEE Press.
- [43] LI, A., SONG, S. L., CHEN, J., LI, J., LIU, X., TALLENT, N. R., AND BARKER, K. J. Evaluating modern gpu interconnect: Pcie, nvlk, nv-sli, nvswitch and gpudirect. *IEEE Transactions on Parallel and Distributed Systems* 31, 1 (2019), 94–110.
- [44] LOVÁSZ, L. Kneser’s conjecture, chromatic number, and homotopy. *Journal of Combinatorial Theory, Series A* 25, 3 (1978), 319–324.
- [45] LU, Y., GU, H., YU, X., AND LI, P. X-nest: A scalable, flexible, and high-performance network architecture for distributed machine learning. *Journal of Lightwave Technology* 39, 13 (2021), 4247–4254.
- [46] MEIJER, P. T. *Connectivities and diameters of circulant graphs*. PhD thesis, Theses (Dept. of Mathematics and Statistics)/Simon Fraser University, 1991.
- [47] MELLETTE, W. M., MCGUINNESS, R., ROY, A., FORENCICH, A., PAPAN, G., SNOEREN, A. C., AND PORTER, G. Rotonet: A scalable, low-complexity, optical datacenter network. In *Proceedings of the Conference of the ACM Special Interest Group on Data Communication* (2017).
- [48] MICROSOFT. Microsoft collective communication library. <https://github.com/microsoft/msccl>, 2022.
- [49] MICROSOFT. Msccl toolkit. <https://github.com/microsoft/msccl-tools>, 2022.
- [50] MILLER, M., AND SIRAN, J. Moore graphs and beyond: A survey of the degree/diameter problem. *Electronic Journal of Combinatorics* 1000 (2013).
- [51] MONAKHOVA, E. A. A survey on undirected circulant graphs. *Discrete Mathematics, Algorithms and Applications* 04, 01 (2012), 1250002.
- [52] NOORDHUIS, P. Accelerating machine learning for computer vision, 2017.
- [53] PATARASUK, P., AND YUAN, X. Bandwidth optimal all-reduce algorithms for clusters of workstations. *Journal of Parallel and Distributed Computing* 69, 2 (2009), 117–124.
- [54] Polatis Optical Circuit Switch. <https://www.polatis.com/series-7000-384x384-port-software-controlled-optical-circuitswitch-sdn-enabled.asp>.
- [55] PORTER, G., STRONG, R., FARRINGTON, N., FORENCICH, A., CHEN-SUN, P., ROSING, T., FAINMAN, Y., PAPAN, G., AND VAHDAT, A. Integrating microsecond circuit switching into the data center. *SIGCOMM Comput. Commun. Rev.* 43, 4 (aug 2013), 447–458.
- [56] SANDERS, P., SPECK, J., AND TRÄFF, J. L. Two-tree algorithms for full bandwidth broadcast, reduction and scan. *Parallel Comput.* 35, 12 (dec 2009), 581–594.
- [57] SERGEEV, A., AND DEL BALSIO, M. Horovod: fast and easy distributed deep learning in tensorflow. *arXiv preprint arXiv:1802.05799* (2018).
- [58] SHAH, A., CHIDAMBARAM, V., COWAN, M., MALEKI, S., MUSUVATHI, M., MYTKOWICZ, T., NELSON, J., SAARIKIVI, O., AND SINGH, R. Synthesizing collective communication algorithms for heterogeneous networks with tacl. *arXiv preprint arXiv:2111.04867* (2021).
- [59] SIMONYAN, K., AND ZISSERMAN, A. Very deep convolutional networks for large-scale image recognition, 2014.
- [60] SINGLA, A., HONG, C.-Y., POPA, L., AND GODFREY, P. B. Jellyfish: Networking data centers randomly. In *9th USENIX Symposium on Networked Systems Design and Implementation (NSDI 12)* (San Jose, CA, Apr. 2012), USENIX Association, pp. 225–238.
- [61] SUZUKI, K., KONOIKE, R., SUDA, S., MATSUURA, H., NAMIKI, S., KAWASHIMA, H., AND IKEDA, K. Low-loss, low-crosstalk, and large-scale optical switch based on silicon photonics. *Journal of Lightwave Technology* 38, 2 (2020), 233–239.
- [62] Telescent G4 Network Topology Manager. <https://www.telescent.com/products>.
- [63] THAKUR, R., RABENSEIFNER, R., AND GROPP, W. Optimization of collective communication operations in MPI. *The International Journal of High Performance Computing Applications* 19, 1 (2005), 49–66.
- [64] TRUONG, T.-N., AND TAKANO, R. Hybrid electrical/optical switch architectures for training distributed deep learning in large-scale. *IEICE Transactions on Information and Systems E104.D*, 8 (2021), 1332–1339.
- [65] UENO, Y., AND YOKOTA, R. Exhaustive study of hierarchical allreduce patterns for large messages between gpus. In *2019 19th IEEE/ACM International Symposium on Cluster, Cloud and Grid Computing (CCGRID)* (2019), pp. 430–439.
- [66] VALADARSKY, A., SHAHAF, G., DINITZ, M., AND SCHAPIRA, M. Xpander: Towards optimal-performance datacenters. In *Proceedings of the 12th International Conference on Emerging Networking Experiments and Technologies* (New York, NY, USA, 2016), CoNEXT '16, Association for Computing Machinery, p. 205–219.
- [67] VALENCIA-PABON, M., AND VERA, J.-C. On the diameter of kneser graphs. *Discrete Mathematics* 305, 1 (2005), 383–385.
- [68] WANG, G., VENKATARAMAN, S., PHANISHAYEE, A., DEVANUR, N., THELIN, J., AND STOICA, I. Blink: Fast and generic collectives for distributed ML. *Proceedings of Machine Learning and Systems* 2 (2020), 172–186.
- [69] WANG, W., KHAZRAEE, M., ZHONG, Z., JIA, Z., MUDIGERE, D., ZHANG, Y., KEWITSCH, A., AND GHOBADI, M. TopoOpt: Optimizing the Network Topology for Distributed DNN Training. *arXiv preprint*

arXiv:2202.00433 (2022).

- [70] WEN, K., SAMADI, P., RUMLEY, S., CHEN, C. P., SHEN, Y., BAHADROI, M., BERGMAN, K., AND WILKE, J. Flexfly: Enabling a reconfigurable dragonfly through silicon photonics. In *Proceedings of the International Conference for High Performance Computing, Networking, Storage and Analysis* (2016), SC '16, IEEE Press.
- [71] WICKRAMASINGHE, U., AND LUMSDAINE, A. A survey of methods for collective communication optimization and tuning, 2016.
- [72] WOODALL, D. R. Sufficient conditions for circuits in graphs. *Proceedings of the London Mathematical Society* 3, 4 (1972), 739–755.
- [73] YEBRA, J. L., FIOLE, M., MORILLO, P., AND ALEGRE, I. The diameter of undirected graphs associated to plane tessellations. *Ars Combinatoria -Waterloo then Winnipeg- 20-B* (01 1985), 159–.
- [74] YOUNG, S., AKSOY, S., FIROZ, J., GIOIOSA, R., HAGGE, T., KEMPTON, M., ESCOBEDO, J., AND RAUGAS, M. Spectrally: Ramanujan graphs as flexible and efficient interconnection networks. In *2022 IEEE International Parallel and Distributed Processing Symposium (IPDPS)* (2022), pp. 1040–1050.
- [75] YU, Y., WU, J., AND HUANG, L. *Double Quantization for Communication-Efficient Distributed Optimization*. Curran Associates Inc., Red Hook, NY, USA, 2019.
- [76] ZHANG, H., ZHENG, Z., XU, S., DAI, W., HO, Q., LIANG, X., HU, Z., WEI, J., XIE, P., AND XING, E. P. Poseidon: An efficient communication architecture for distributed deep learning on gpu clusters. In *Proceedings of the 2017 USENIX Conference on Usenix Annual Technical Conference (USA, 2017), USENIX ATC '17*, USENIX Association, p. 181–193.
- [77] ZHU, Z., TEH, M. Y., WU, Z., GLICK, M. S., YAN, S., HATTINK, M., AND BERGMAN, K. Distributed deep learning training using silicon photonic switched architectures. *APL Photonics* 7, 3 (2022), 030901.

A Reduce-Scatter & Allgather

DEFINITION 7 (REDUCE-SCATTER). *An algorithm (G, A) is a reduce-scatter algorithm if for arbitrary $x \in S$ and distinct $u, v \in V_G$, there exists a sequence in A :*

$$\begin{aligned} &((v, C_1), (w_0, w_1), t_1), ((v, C_2), (w_1, w_2), t_2), \dots \\ &((v, C_n), (w_{n-1}, w_n), t_n), \end{aligned}$$

where $w_0 = u, w_n = v, t_1 < t_2 < \dots < t_n$, and $x \in C_1 \cap C_2 \cap \dots \cap C_n$.

An allgather algorithm has the same definition except $w_0 = v$ and $w_n = u$.

In this paper, many of the techniques are discussed under either reduce-scatter or allgather only. We will show that anything holds in either reduce-scatter or allgather has an equivalent version for the other collective operation.

DEFINITION 8 (REVERSE SCHEDULE). *A reverse schedule A^T of A is a schedule for transpose graph G^T such that $((w, C), (v, u), t_{\max} - t + 1) \in A^T$ iff $((w, C), (u, v), t) \in A$, where t_{\max} is the maximum comm step in A .*

It is trivial to see that $T_L(A) = T_L(A^T)$ and $T_B(A) = T_B(A^T)$.

THEOREM 1. *If A is a reduce-scatter/allgather schedule on G , then A^T is an allgather/reduce-scatter schedule on G^T .*

PROOF. Suppose (G, A) is a reduce-scatter algorithm. For arbitrary $x \in S$ and distinct $u, v \in V_G$, there exists a sequence of tuples in A :

$$\begin{aligned} &((v, C_1), (w_0, w_1), t_1), ((v, C_2), (w_1, w_2), t_2), \dots \\ &((v, C_n), (w_{n-1}, w_n), t_n), \end{aligned}$$

where $w_0 = u, w_n = v, t_1 < t_2 < \dots < t_n$, and $x \in C_1 \cap C_2 \cap \dots \cap C_n$. It follows that there exists a sequence of tuples in A^T :

$$\begin{aligned} &((v, C_n), (w_n, w_{n-1}), t'_n), \dots \\ &((v, C_2), (w_2, w_1), t'_2), ((v, C_1), (w_1, w_0), t'_1). \end{aligned}$$

where $t'_i = t_{\max} - t_i + 1$, so $t'_n < \dots < t'_2 < t'_1$. Since u, v, x are arbitrary, A^T is an allgather schedule on G^T . One can similarly show that if (G, A) is an allgather algorithm, then (G^T, A^T) is a reduce-scatter algorithm. \square

Theorem 1 has the following two corollaries:

COROLLARY 1. *Suppose $f : G \mapsto A$ is a function to construct reduce-scatter/allgather schedule on G , then $g : G \mapsto f(G^T)^T$ is a function to construct allgather/reduce-scatter schedule on G .*

COROLLARY 2. *Suppose $f : (G, A) \mapsto (f(G), f(A))$ is a mapping within reduce-scatter/allgather algorithms, then $g : (G, A) \mapsto (f(G^T)^T, f(A^T)^T)$ is a mapping within allgather/reduce-scatter algorithms.*

For example, the line graph expansion in §4.1 can be seen as a mapping within reduce-scatter, and the linear program (1) can be seen as a function to construct reduce-scatter schedule. Thus, corollary 1 and 2 have shown that they both have a equivalent version in allgather.

In undirected topology, it is well-known that reduce-scatter and allgather is a pair of dual operation such that one can be transformed into another by reversing the communication [20]. It is similar in directed topology but with additional requirement and more complicated transformation.

DEFINITION 9 (SCHEDULE ISOMORPHISM). *Suppose G and G' are isomorphic. Let $f : V_G \rightarrow V_{G'}$ be the graph isomorphism, then $f(A)$ is a schedule for G' such that $((f(w), C), (f(u), f(v)), t) \in f(A)$ iff $((w, C), (u, v), t) \in A$.*

THEOREM 2. *Suppose G is skew-symmetric. Let G^T be the transpose graph, and let $f : V_{G^T} \rightarrow V_G$ be the isomorphism from G^T to G . If (G, A) is a reduce-scatter/allgather algorithm, then $(G, f(A^T))$ is an allgather/reduce-scatter algorithm with $T_L(A) = T_L(f(A^T))$ and $T_B(A) = T_B(f(A^T))$.*

PROOF. By definition of $f(A^T)$,

$$\begin{aligned} ((f(v), C), (f(u'), f(u)), t_{\max} - t + 1) &\in f(A^T) \\ &\Leftrightarrow ((v, C), (u', u), t_{\max} - t + 1) \in A^T \\ &\Leftrightarrow ((v, C), (u, u'), t) \in A. \end{aligned}$$

Note that $(u, u') \in E_G \Leftrightarrow (u', u) \in E_{G^T} \Leftrightarrow (f(u'), f(u)) \in E_G$, so $f(A^T)$ is a valid schedule for G .

Suppose (G, A) is a reduce-scatter algorithm. For arbitrary $x \in S$ and distinct $u, v \in V_G$, there exists a sequence of tuples in A :

$$\begin{aligned} ((v, C_1), (w_0, w_1), t_1), ((v, C_2), (w_1, w_2), t_2), \dots \\ ((v, C_n), (w_{n-1}, w_n), t_n), \end{aligned}$$

where $w_0 = u, w_n = v, t_1 < t_2 < \dots < t_n$, and $x \in C_1 \cap C_2 \cap \dots \cap C_n$. It follows that there exists a sequence of tuples in $f(A^T)$:

$$\begin{aligned} ((f(v), C_n), (f(w_n), f(w_{n-1})), t_{\max} - t_n + 1), \\ ((f(v), C_{n-1}), (f(w_{n-1}), f(w_{n-2})), t_{\max} - t_{n-1} + 1), \\ \vdots \\ ((f(v), C_1), (f(w_1), f(w_0)), t_{\max} - t_1 + 1), \end{aligned}$$

where $f(w_0) = f(u), f(w_n) = f(v), t_{\max} - t_n + 1 < t_{\max} - t_{n-1} + 1 < \dots < t_{\max} - t_1 + 1$, and $x \in C_n \cap C_{n-1} \cap \dots \cap C_1$. Because f is a bijection, $(G, f(A^T))$ is an allgather algorithm. $T_L(A) = T_L(f(A^T))$ and $T_B(A) = T_B(f(A^T))$ are trivial, and one can similarly prove that if (G, A) is an allgather algorithm, then $(G, f(A^T))$ is a reduce-scatter algorithm. \square

What theorem 2 has established is that given any skew-symmetric topology, if we have either one of reduce-scatter

and allgather algorithm, then we have both reduce-scatter and allgather. Since allreduce can be achieved by applying a reduce-scatter followed by an allgather, we only need to come up with a reduce-scatter or allgather to construct a complete allreduce algorithm. Furthermore, if we have a reduce-scatter or allgather algorithm with runtime T , then we have an allreduce algorithm with runtime $2T$.

B Optimality

Because our cost model is only concerned with node latency and bandwidth runtime, the optimality of reduce-scatter/allgather algorithm is only related to node latency optimality and bandwidth optimality in this paper.

B.1 Node Latency Optimality

DEFINITION 10 (NODE LATENCY OPTIMAL). *Given an N -node reduce-scatter/allgather algorithm (G, A) , if any other N -node reduce-scatter/allgather algorithm (G', A') satisfies $T_L(A') \geq T_L(A)$, then (G, A) is node latency optimal.*

THEOREM 3. *For any reduce-scatter/allgather algorithm (G, A) , it holds that $T_L(A)/\alpha \geq D(G)$, where $D(G)$ is the diameter of G .*

PROOF. The proof is trivial. \square

Because we can always construct a SPFF schedule A for topology G with $T_L(A)/\alpha = D(G)$, it follows the corollary:

COROLLARY 3. *An N -node reduce-scatter/allgather algorithm (G, A) is node latency optimal if and only if*

$$T_L(A)/\alpha = D(G) = \min_{G': |V_{G'}|=N} D(G').$$

The minimum diameter of a regular directed graph with a given number of vertices and degree is still an open question. One can check *degree/diameter problem* for more information [50]. However, the Moore bound for digraph is sufficient to tell the node latency optimality in most cases.

DEFINITION 11 (MOORE OPTIMAL). *Let (G, A) be an N -node reduce-scatter/allgather algorithm with $T_L(A) = \alpha k$, then (G, A) is Moore optimal if and only if $N > M_{d,k-1}$, where $M_{d,k-1}$ is the Moore bound of degree d and diameter $k-1$.*

Because for any d -regular graph $G, D(G) \geq k$ as long as $|V_G| > M_{d,k-1}$, Moore optimality is a stronger condition than node latency optimality. We define a function T_L^* such that $T_L^*(N)$ is equal to the Moore optimal node latency of N -node reduce-scatter/allgather algorithms.

B.2 Bandwidth Optimality

DEFINITION 12 (BANDWIDTH OPTIMAL). *Given an N -node reduce-scatter/allgather algorithm (G, A) , if any other N -node reduce-scatter/allgather algorithm (G', A') satisfies $T_B(A') \geq T_B(A)$, then (G, A) is bandwidth optimal.*

THEOREM 4. $\frac{M}{B} \cdot \frac{N-1}{N}$ is a lower bound of $T_B(A)$ for any N -node reduce-scatter/allgather algorithm (G, A) .

PROOF. In reduce-scatter/allgather, each node needs to either send at least $M \cdot \frac{N-1}{N}$ amount of data. Thus, the minimum bandwidth runtime is $\frac{M}{B} \cdot \frac{N-1}{N}$. \square

Because it is trivial to construct a schedule A with $T_B(A) = \frac{M}{B} \cdot \frac{N-1}{N}$ for an unidirectional ring of size N , it follows the corollary:

COROLLARY 4. *An N -node reduce-scatter/allgather algorithm (G, A) is bandwidth optimal if and only if*

$$T_B(A) = \frac{M}{B} \cdot \frac{N-1}{N}.$$

Thus, we define a function T_B^* such that $T_B^*(N) = \frac{M}{B} \cdot \frac{N-1}{N}$ is the optimal bandwidth runtime of N -node reduce-scatter/allgather algorithms.

From corollary 4, we have the following necessary and sufficient condition for bandwidth optimality.

THEOREM 5. *A reduce-scatter/allgather algorithm (G, A) is bandwidth optimal if and only if:*

- (1) $\frac{1}{B/d} \sum_{((w,C),(u,v)) \in A_t} |C| = T_B(A_t)$ for all $(u, v) \in E_G$ and $t \in \{1, \dots, t_{\max}\}$,
- (2) Pick any distinct $u, w \in V_G$. For each $x \in S$, there exists a unique $((w, C), (u, v), t) \in A$ such that $x \in C$.

PROOF. If $T_B(A) = T_B^*(N)$, then the amount of data sent out by each vertex must be equal to $M \cdot \frac{N-1}{N}$. Thus, if (G, A) is bandwidth optimal, (2) must hold. If (1) does not hold, there exists some link (u, v) not fully utilized at some comm step. Because part of the bandwidth of (u, v) is wasted, $T_B(A) > T_B^*(N)$.

If (1) and (2) hold, then every vertex send/receive exactly $M \cdot \frac{N-1}{N}$ in total and bandwidth are fully utilized. Thus, $T_B(A) = T_B^*(N)$ and (G, A) is bandwidth optimal. \square

B.3 Allreduce Optimality

In this paper, we construct an allreduce algorithm through a reduce-scatter followed by allgather. In such construction, the lower bound of allreduce algorithm is $2(T_L^*(N) + T_B^*(N))$. To compare this with the lower bound of any allreduce construction, in [53], the authors have proved that $2T_B^*(N)$ is indeed the lower bound of bandwidth runtime of any allreduce algorithm. As for node latency, a reduce-scatter followed by allgather has at least $2D(G)$ number of comm steps, so $2T_L^*(N)$ is the lower bound of node latency. Indeed, one can use all-to-all to construct an allreduce with number of comm steps equal to one diameter $D(G)$ (lower bound being $T_L^*(N)$ instead of $2T_L^*(N)$). However, the lower bound of bandwidth runtime for all-to-all is $\frac{M}{B} \cdot (N-1) = N \cdot T_B^*(N)$, which is much worse than $2T_B^*(N)$.

There is also another way of constructing allreduce with reduce followed by broadcast as in double binary tree [38, 56]. In such an approach, the number of comm steps can be

twice the radius of G instead of twice the diameter. However, the Moore bound for graph diameter also applies to graph radius, so $2T_L^*(N)$ is still a lower bound of allreduce via reduce+broadcast. Because of theorem 14, the optimal allreduce via reduce+broadcast is at most 2α faster than generalized Kautz graph can do with reduce-scatter followed by allgather. Furthermore, reduce+broadcast is also poor in bandwidth runtime. In double binary tree, each link of the root has to at least receive $M/2$ in reduce stage and send $M/2$ in broadcast stage, so the bandwidth runtime is at least¹ $2 \cdot \frac{M/2}{B/4} \geq 4T_B^*(N)$ even with pipelining. Although one can improve this bound by superpositioning more trees, such an improvement inevitably increases the degree of topology and degrades node latency.²

C Computational Cost

In this paper, we have omitted the computational cost of reduction operation in performance analysis. While this approach is commonly adopted in previous literature [18, 56, 58, 68], we give a formal reasoning why this approach is legitimate. It is not only because computational cost is generally orders of magnitude lower than network cost, but also because computational cost can be incorporated into network cost.

Assume a cost model where computation and network communication do not overlap at each node. In particular, at each comm step of reduce-scatter, the computation to reduce chunks happens immediately after the node receives all chunks and before the node starts to send out chunks for the next comm step. We adopt notation from [20], where γ denotes the computational time cost per size of data. Like node latency and bandwidth runtime, we also let $T_C(A)$ be the total time spent on computation by schedule A . As argued in [20], a lower bound of computational cost is $T_C \geq M \cdot \gamma \cdot \frac{N-1}{N}$ for both reduce-scatter and allreduce, which is identical to the bandwidth optimality of reduce-scatter and half of the bandwidth optimality of allreduce. The following theorem shows that bandwidth runtime of a schedule can somewhat also act as an upper bound for the computational time.

THEOREM 6. *Given a reduce-scatter algorithm (G, A) , suppose $T_B(A) = \frac{M}{B} \cdot y$, then $T_C(A) \leq M \cdot \gamma \cdot y$.*

PROOF. At any comm step t , suppose the bandwidth runtime $T_B(A_t) = \frac{M}{B} \cdot y_t$. It follows at comm step t , each link of G transmits at most $\frac{B}{d} \cdot \frac{M}{B} \cdot y_t = \frac{M}{d} \cdot y_t$ amount of data. Since each node has d incoming edges, the amount of data each node receives is at most $d \cdot \frac{M}{d} \cdot y_t = M \cdot y_t$ and thus $T_C(A_t) \leq M \cdot \gamma \cdot y_t$. The theorem trivially follows $y = \sum_t y_t$. \square

¹We regard double binary tree as a degree 4 topology.

² $T_L^*(N)$ decreases as degree increases.

With theorem 6, if we have proven the bandwidth runtime of some allreduce schedule A is $T_B(A) = 2\frac{M}{B} \cdot y$, then $T_B(A) + T_C(A) \leq M \cdot (\frac{2}{B} + \gamma) \cdot y$, in which $T_B(A) + T_C(A)$ is the only part of runtime growing as data size M grows. We can thus simply define $B' = (\frac{1}{B} + \frac{\gamma}{2})^{-1}$, and then $2\frac{M}{B'} \cdot y$ can represent the sum of bandwidth runtime and computational runtime all together. The value of y is all that matters. The following corollary shows that if an algorithm is bandwidth optimal, then such representation is exact.

COROLLARY 5. *If allreduce algorithm (G, A) is bandwidth optimal i.e. $T_B(A) = 2T_B^*(N) = 2\frac{M}{B} \cdot \frac{N-1}{N}$, then $T_C(A) = M \cdot \gamma \cdot \frac{N-1}{N}$ and $T_B(A) + T_C(A) = 2M \cdot (\frac{1}{B} + \frac{\gamma}{2}) \cdot \frac{N-1}{N}$.*

When profiling a testbed, one can simply derive the value of $\frac{1}{B} + \frac{\gamma}{2}$ using bandwidth optimal topologies and use it as $1/B$ to apply the results of this paper. While it is still possible for two schedules having the same bandwidth performance to have different computational runtimes, such difference is both bounded by the aforementioned theorems and minimal compared to bandwidth runtime which is order of magnitude greater.

D Optimality Analysis of Expansion Techniques

In this section, we provide proofs for the node latency and bandwidth optimality properties of the various expansion techniques.

D.1 Line Graph Expansion

DEFINITION 1 (LINE GRAPH). *Given a directed graph (or digraph) G , each edge $(u, v) \in E_G$ corresponds to a vertex uv in the line graph $L(G)$. Vertex uu' is connected to vv' in digraph $L(G)$ if and only if $u' = v$.*

DEFINITION 2 (SCHEDULE OF LINE GRAPH). *Given a reduce-scatter schedule A_G for topology G , let $A_{L(G)}$ be the schedule for line graph $L(G)$ containing:*

1. $((vv', C), (wu, uu'), t)$ for all $((v, C), (u, u'), t) \in A_G$ and distinct $(v, v'), (w, u) \in E_G$;
2. $((vv', S), (uv, vv'), t_{\max} + 1)$ for all $(uv, vv') \in E_{L(G)}$ with $uv \neq vv'$. t_{\max} is the maximum comm step in A_G .

THEOREM 7. *Given a d -regular topology G , if (G, A_G) is an N -node reduce-scatter algorithm with $T_B(A_G, M, B) = \tau(M/B)$ for some constant τ ,³ then $(L(G), A_{L(G)})$ is a dN -node reduce-scatter algorithm satisfying:*

$$T_L(A_{L(G)}) = T_L(A_G) + \alpha, \quad (3)$$

$$T_B(A_{L(G)}) \leq T_B(A_G) + \frac{M}{B} \cdot \frac{1}{N}. \quad (4)$$

PROOF. Let wu, vv' be arbitrary two distinct vertices in $L(G)$. We want to show there exists a sequence in $A_{L(G)}$

³The assumption $T_B(A_G, M, B) = \tau(M/B)$ for some constant τ almost always holds. One would reasonably assume the bandwidth runtime is linear in model size and the inverse of bandwidth.

going from wu to vv' like in definition 7 for any $x \in S$. If $u = v$, then $((vv', S), (wu, vv'), t_{\max} + 1)$ at the last comm step suffices. If $u \neq v$, because A_G is reduce-scatter, there exists a sequence in A_G :

$$\begin{aligned} &((v, C_1), (u, w_1), t_1), ((v, C_2), (w_1, w_2), t_2), \dots \\ &((v, C_n), (w_{n-1}, v), t_n), \end{aligned}$$

where $t_1 < t_2 < \dots < t_n$ and $x \in C_1 \cap C_2 \cap \dots \cap C_n$. Thus, by definition 2, there exists a sequence in $A_{L(G)}$:

$$\begin{aligned} &((vv', C_1), (wu, uw_1), t_1), \\ &\quad \vdots \\ &((vv', C_n), (w_{n-2}w_{n-1}, w_{n-1}v), t_n), \\ &((vv', S), (w_{n-1}v, vv'), t_{\max} + 1), \end{aligned}$$

as desired. The new algorithm $(L(G), A_{L(G)})$ has dM total data length, because the number of nodes has grown d -fold while the size of a shard remains the same.

As for $T_L(A_{L(G)})$ and $T_B(A_{L(G)})$, equality (3) trivially follows the definition 2. Let $[A_{L(G)}]_t$ and $[A_G]_t$ be the subschedules of $A_{L(G)}$ and A_G at comm step t . Given $v \in V_G$, because G is d -regular, we have $|\{(v, v') \mid (v, v') \in E_G\}| = d$. Given any edge (wu, uu') and $t \leq t_{\max}$, there are at most d number of $((vv', C), (wu, uu'), t) \in A_{L(G)}$ for each $((v, C), (u, u'), t) \in A_G$ by definition 2. Thus,

$$\sum_{((vv', C), (wu, uu')) \in [A_{L(G)}]_t} |C| \leq \sum_{((v, C), (u, u')) \in [A_G]_t} d \cdot |C|.$$

It follows that $T_B([A_{L(G)}]_t, dM, B) \leq d \cdot T_B([A_G]_t, M, B)$ and hence $\sum_{t=1}^{t_{\max}} T_B([A_{L(G)}]_t, dM, B) \leq d \cdot T_B(A_G, M, B)$. For the last comm step $t_{\max} + 1$, we have

$$T_B([A_{L(G)}]_{t_{\max}+1}, dM, B) = \frac{|S|}{B/d} = \frac{M/N}{B/d}.$$

Since $T_B(A_G, M, B) = \tau(M/B)$ for some constant τ , we have $d \cdot T_B(A_G, M, B) = T_B(A_G, dM, B)$. It follows that

$$\begin{aligned} T_B(A_{L(G)}, dM, B) &= \sum_{t=1}^{t_{\max}+1} T_B([A_{L(G)}]_t, dM, B) \\ &\leq d \cdot T_B(A_G, M, B) + \frac{M/N}{B/d} = T_B(A_G, dM, B) + \frac{dM}{B} \cdot \frac{1}{N}. \end{aligned}$$

Replacing dM by M gives (4) as desired. \square

COROLLARY 6. *Given a d -regular topology G , if (G, A_G) is an N -node reduce-scatter algorithm with $T_B(A_G, M, B) = \tau(M/B)$ for some constant τ , then $(L^n(G), A_{L^n(G)})$ is a $d^n N$ -node reduce-scatter algorithm satisfying:*

$$T_L(A_{L^n(G)}) = T_L(A_G) + n\alpha, \quad (5)$$

$$T_B(A_{L^n(G)}) \leq T_B(A_G) + \frac{M}{B} \cdot \frac{d}{d-1} \left(\frac{1}{|V_G|} - \frac{1}{|V_{L^n(G)}|} \right). \quad (6)$$

THEOREM 8. $(L^n(G), A_{L^n(G)})$ is Moore optimal if and only if (G, A_G) is Moore optimal.

PROOF. Suppose $T_L(A_G) = \alpha k$. Thus, (G, A_G) is Moore optimal if and only if

$$N > M_{d,k-1} = \sum_{i=0}^{k-1} d^i = \frac{d^k}{d-1} - \frac{1}{d-1}. \quad (7)$$

$(L^n(G), A_{L^n(G)})$ is Moore optimal if and only if

$$d^n N > M_{d,k+n-1} \Leftrightarrow N > \frac{d^k}{d-1} - \frac{1}{d^n(d-1)}. \quad (8)$$

Because $(8) - (7) < 1$ and (7) is an integer, (7) and (8) are equivalent. \square

THEOREM 9. If (G, A_G) is bandwidth optimal with N nodes, then $T_B(A_{L^n(G)})/T_B^*(|V_{L^n(G)}|) \leq 1 + [(d-1)N]^{-1}$ for all n .

PROOF. If (G, A_G) is bandwidth optimal, then (6) gives:

$$T_B(A_{L^n(G)}) \leq \frac{M}{B} \left[1 + \frac{1}{d-1} \left(\frac{1}{N} - \frac{d}{d^n N} \right) \right]. \quad (9)$$

It is trivial to see that $(9)/T_B^*(d^n N) \nearrow 1 + [(d-1)N]^{-1}$ as $n \rightarrow \infty$. \square

THEOREM 10. Let A_G be a SPFF reduce-scatter schedule on G with $|N^-(u)| > 1$ for all $u \in V_G$, then the expanded schedule $A_{L(G)}$ is a SPFF reduce-scatter schedule on $L(G)$. In particular, if A_G is the optimal SPFF schedule on G , then $A_{L(G)}$ is the optimal SPFF schedule on $L(G)$ satisfying:

$$T_B(A_{L(G)}) = T_B(A_G) + \frac{M}{B} \cdot \frac{1}{N}. \quad (10)$$

PROOF. It is trivial to see that $A_{L(G)}$ is a SPFF reduce-scatter schedule on $L(G)$ by property (2) in §4.1. For the sake of contradiction, suppose there exists a SPFF schedule $A'_{L(G)}$ that $T_B(A'_{L(G)}) < T_B(A_G) + \frac{M}{B} \cdot \frac{1}{N}$. Let $x_{wu,uu',vv',t}^*$ be the solution of (1) corresponding to $A'_{L(G)}$. We build a schedule A'_G by constructing a solution of (1) such that

$$x_{u,u',v,t} = \frac{1}{d} \sum_{(v,v')} x_{wu,uu',vv',t}^*$$

where $w \in N^-(u) \setminus \{v\}$ is arbitrary. To verify the construction is a valid solution, given any $u \in V_G$ and $v \in N_{D(G)+1-t}^G(u)$, the equality of (1) follows:

$$\begin{aligned} \sum_{(u,u')} x_{u,u',v,t} &= \frac{1}{d} \sum_{(v,v')} \sum_{(u,u')} x_{wu,uu',vv',t}^* \\ &= \frac{1}{d} \sum_{(v,v')} \sum_{(wu,uu')} x_{wu,uu',vv',t}^* = \frac{1}{d} \sum_{(v,v')} 1 = \frac{1}{d} \cdot d = 1. \end{aligned}$$

The second equality follows property (2) in §4.1, and the third equality follows the equality constraint in (1). Now, given $(u, u') \in E_G$, observe that

$$\begin{aligned} \sum_v x_{u,u',v,t} &= \frac{1}{d} \sum_v \sum_{(v,v')} x_{wu,uu',vv',t}^* \\ &= \frac{1}{d} \sum_{vv'} x_{wu,uu',vv',t}^* \leq \frac{1}{d} U_{wu,t}. \end{aligned}$$

Thus, it holds that $U_{u,t} = \max_{u'} \sum_v x_{u,u',v,t} \leq \frac{1}{d} U_{wu,t}$ and hence

$$\max_{u \in V_G} U_{u,t} \leq \frac{1}{d} \max_{wu \in V_{L(G)}} U_{wu,t}.$$

Given $N = |V_G|$, by (2), we have

$$\begin{aligned} T_B(A'_G) &\leq T_B(A'_{L(G)}) - \frac{M/(dN)}{B/d} \\ &= T_B(A'_{L(G)}) - \frac{M}{B} \cdot \frac{1}{N} < T_B(A_G), \end{aligned}$$

contradicting A_G being the optimal SPFF schedule. Thus, combined with inequality (4), we have proven $A_{L(G)}$ being optimal as well as the equality (10). \square

COROLLARY 7. Let A_G be a SPFF reduce-scatter schedule on G with $|N^-(u)| > 1$ for all $u \in V_G$, then the expanded schedule $A_{L^n(G)}$ is a SPFF reduce-scatter schedule on $L^n(G)$. In particular, if A_G is the optimal SPFF schedule on G , then $A_{L^n(G)}$ is the optimal SPFF schedule on $L^n(G)$ satisfying:

$$T_B(A_{L^n(G)}) = T_B(A_G) + \frac{M}{B} \cdot \frac{d}{d-1} \left(\frac{1}{|V_G|} - \frac{1}{|V_{L^n(G)}|} \right). \quad (11)$$

D.2 Degree Expansion

DEFINITION 3 (DEGREE EXPANDED TOPOLOGY). Given a topology G without self-loops and $n \in \mathbb{N}$, construct the degree expanded topology $G * n$ such that

1. For each vertex $v \in V_G$, add v_1, \dots, v_n to V_{G*n} ,
2. For each edge $(u, v) \in E_G$, add (u_i, v_j) to E_{G*n} for all i, j including $i = j$.

DEFINITION 4 (DEGREE EXPANDED SCHEDULE). Given a reduce-scatter schedule A_G for G , construct A_{G*n} for $G * n$:

1. Divide shard S into equal-sized chunks C_1, \dots, C_{nd} . For each $u_i, u_j \in V_{G*n}$ with $i \neq j$ and for each $(u_i, v_1), \dots, (u_i, v_{nd}) \in E_{G*n}$, add $((u_i, C_\alpha), (u_i, v_\alpha), 1)$ to A_{G*n} .
2. For all i, j including $i = j$ and for each $((w, C), (u, v), t)$ in A_G , add $((w_j, C), (u_i, v_j), t + 1)$ to A_{G*n} .

THEOREM 11. Given a d -regular topology G without self-loops, if (G, A_G) is an N -node reduce-scatter algorithm with $T_B(A_G, M, B) = \tau(M/B)$ for some constant τ , then $(G*n, A_{G*n})$

is an nN -node reduce-scatter algorithm satisfying:

$$T_L(A_{G*n}) = T_L(A_G) + \alpha, \quad (12)$$

$$T_B(A_{G*n}) = T_B(A_G) + \frac{M}{B} \cdot \frac{n-1}{nN}. \quad (13)$$

PROOF. Let u_i, v_j be arbitrary two distinct vertices in $G * n$. Suppose $u \neq v$ in G , then for any $x \in S$, there exists a sequence in A_G :

$$\begin{aligned} & ((v, C_1), (u, w^{(1)}), t_1), ((v, C_2), (w^{(1)}, w^{(2)}), t_2), \dots \\ & ((v, C_n), (w^{(n-1)}, v), t_n), \end{aligned}$$

where $t_1 < t_2 < \dots < t_n$ and $x \in C_1 \cap C_2 \cap \dots \cap C_n$. By definition 4, there exists a sequence in A_{G*n} :

$$\begin{aligned} & ((v_j, C_1), (u_i, w_j^{(1)}), t_1+1), ((v_j, C_2), (w_j^{(1)}, w_j^{(2)}), t_2+1), \dots \\ & ((v_j, C_n), (w_j^{(n-1)}, v_j), t_n+1), \end{aligned}$$

as desired. Now, suppose $u = v$ in G , then in first step of definition 4, x has been send to some neighbor u'_k of u_i . Since $u' \neq v$, by previous proof, we can find a sequence taking x from u'_k to v_j . Thus, there exists a sequence in A_{G*n} taking x from u_i to u'_k and then to v_j , so A_{G*n} is a reduce-scatter algorithm.

From second step of definition 4, it is easy to see that $T_B([A_{G*n}]_{t+1}, nM, nB) = T_B([A_G]_t, M, B)$ and hence $\sum_{t=2}^{t_{\max}+1} T_B([A_{G*n}]_t, nM, nB) = T_B(A_G, M, B)$. The nM and nd are due to the fact that both the number of nodes and degree have grown n -fold. Thus, we have

$$\begin{aligned} T_B(A_{G*n}, nM, nB) &= T_B(A_G, M, B) + T_B([A_{G*n}]_1, M, B) \\ &= T_B(A_G, M, B) + (n-1) \cdot \frac{(nM)/(nN)}{nd} \cdot \frac{1}{nB/(nd)} \\ &= T_B(A_G, M, B) + \frac{M}{B} \cdot \frac{n-1}{nN}. \end{aligned}$$

(13) trivially follows the assumption that $T_B(A_G, M, B) = \tau(M/B)$ for some constant τ . \square

COROLLARY 8. If (G, A_G) is bandwidth optimal and $T_B(A_G, M, B) = \tau(M/B)$ for some constant τ , then $(G*n, A_{G*n})$ is bandwidth optimal.

THEOREM 12 (SPFF DEGREE EXPANSION). Given the same degree expanded topology, the SPFF LP (1) gives $T_L(A_{G*n}) = T_L(A_G)$ and $T_B(A_{G*n}) = T_B(A_G) + \frac{M}{B} \cdot \frac{n-1}{nN}$ if the following holds:

- (1) A_G is a SPFF schedule,
- (2) $d(u_i, u_j)$ s are equal for all u and $i \neq j$, i.e., the shortest cycle (not necessarily an edge-disjoint one) including a given vertex has the same length for all vertices in G .⁴

⁴Note that all bidirectional topologies trivially satisfy this requirement with the shortest cycles having length 2.

PROOF. Note that if A_G is a SPFF schedule, then all traffic in A_{G*n} except the u_i -to- u_j ones follow the shortest paths in $G * n$. If these two conditions hold, instead of creating a new comm step 1 in 1. of definition 4, one can add all u_i -to- u_j traffic to comm step $D(G) - d(u_i, u_j) + 1$ with $((u_j, C_\alpha), (u_i, v_\alpha), D(G) - d(u_i, u_j) + 1)$. Thus, the resulting schedule A_{G*n} is SPFF, and no new comm step is created, so $T_L(A_{G*n}) = T_L(A_G)$. \square

D.3 Cartesian Power Expansion

DEFINITION 5 (CARTESIAN PRODUCT). The Cartesian product digraph $G_1 \square G_2$ of digraphs G_1 and G_2 has vertex set $V_{G_1} \times V_{G_2}$ with vertex $\mathbf{u} = (u_1, u_2)$ connected to $\mathbf{v} = (v_1, v_2)$ iff either $(u_1, v_1) \in E_{G_1}$ and $u_2 = v_2$; or $u_1 = v_1$ and $(u_2, v_2) \in E_{G_2}$.

DEFINITION 13 (SCHEDULE OF CARTESIAN POWER). Given an allgather schedule A_G for topology G and $n \in \mathbb{N}$, construct the schedule $A_{G^{\square n}}$ for $G^{\square n}$:

1. Construct the schedule $A^{(1)}$:
2. For $j = 1, \dots, n$, for each $((w, C), (u, v), t) \in A_G$, add

$$(((\mathbf{x}, w, \mathbf{z}), C), ((\mathbf{y}, u, \mathbf{z}), (\mathbf{y}, v, \mathbf{z}))), t + (j-1)t_{\max})$$

to $A^{(1)}$ for all $\mathbf{x}, \mathbf{y} \in V_G^{j-1}$ and $\mathbf{z} \in V_G^{n-j}$. t_{\max} is the maximum comm step in A_G .

3. Similarly, construct $A^{(i)}$ for $i = 2, \dots, n$ such that each vertex \mathbf{v} in $A^{(i)}$ is shifted by $i-1$ to $(\mathbf{v}[n-i+2:n], \mathbf{v}[1:n-i+1])$.
4. Divide each shard into n subshards. Construct schedule $A_{G^{\square n}}$ such that $A^{(i)}$ performs allgather over the i th subshards of all nodes.

THEOREM 13. Given a d -regular topology G , if (G, A_G) is an N -node allgather algorithm with $T_B(A_G, M, B) = \tau(M/B)$ for some constant τ , then $G^{\square n}$ is an nd -regular topology, and $(G^{\square n}, A_{G^{\square n}})$ is an N^n -node allgather algorithm satisfying:

$$T_L(A_{G^{\square n}}) = n \cdot T_L(A_G), \quad (14)$$

$$T_B(A_{G^{\square n}}) = T_B(A_G) \cdot \frac{N}{N-1} \cdot \frac{N^n - 1}{N^n}. \quad (15)$$

PROOF. We have already shown that $A_{G^{\square n}}$ is a valid allgather schedule for $G^{\square n}$, and (14) is trivial. To prove (15), observe that at each j , the total size of data needs to be allgathered at each subgraph $H_{u,i}$ is $N^{j-1}M/n$. It follows that

$$\begin{aligned} T_B(A^{(i)}, N^{n-1}M/n, nB) &= \sum_{j=1}^n T_B(A_G, N^{j-1}M/n, nB) \\ &= \sum_{j=1}^n \frac{N^{j-1}}{n^2} T_B(A_G, M, B) \\ &= \frac{N^n - 1}{n^2(N-1)} T_B(A_G, M, B). \end{aligned}$$

Again, by assumption $T_B(A_G, M, B) = \tau(M/B)$, we have

$$\begin{aligned} T_B(A_{G^{\square n}}, M, B) &= \sum_{i=1}^n T_B(A^{(i)}, M/n, B) \\ &= \sum_{i=1}^n \frac{n}{N^{n-1}} T_B(A^{(i)}, N^{n-1}M/n, nB) \\ &= n \cdot \frac{n}{N^{n-1}} \cdot \frac{N^n - 1}{n^2(N-1)} \cdot T_B(A_G, M, B) \\ &= T_B(A_G, M, B) \cdot \frac{N}{N-1} \cdot \frac{N^n - 1}{N^n}. \end{aligned}$$

□

We then have the following corollary.

COROLLARY 9. *If (G, A_G) is bandwidth optimal and $T_B(A_G, M, B) = \tau(M/B)$ for some constant τ , then $(G^{\square n}, A_{G^{\square n}})$ is bandwidth optimal.*

THEOREM 14. *Let $(G_1, A_{G_1}), \dots, (G_n, A_{G_n})$ be reduce-scatter algorithms such that*

- (1) G_1, \dots, G_n are nontrivial simple digraphs;
- (2) A_{G_1}, \dots, A_{G_n} are bandwidth optimal SPFF schedules.

The optimal SPFF schedule (i.e., schedule given by (1)) $A_{G_1 \square \dots \square G_n}$ on $G_1 \square \dots \square G_n$ is also bandwidth optimal.

PROOF. To prove the theorem, it is sufficient to show that if G_1 and G_2 have bandwidth optimal SPFF schedules, then $G_1 \square G_2$ has bandwidth optimal SPFF schedule. By theorem 19, let x_{u_1, w_1, v_1, t_1}^* and x_{u_2, w_2, v_2, t_2}^* be the solutions of (1) on G_1 and G_2 respectively. Let $\mathbf{u} = (u_1, u_2)$ and $\mathbf{v} = (v_1, v_2)$. Define a value $r \in [0, 1]$ which we will decide later. We construct a solution of (1) for $G_1 \square G_2$ such that:

$$\begin{aligned} x_{\mathbf{u}, (w_1, u_2), \mathbf{v}, t_1+t_2-1} &= \begin{cases} r \cdot x_{u_1, w_1, v_1, t_1}^* & \text{if } u_2 \neq v_2, \\ x_{u_1, w_1, v_1, t_1}^* & \text{if } u_2 = v_2, \end{cases} \\ x_{\mathbf{u}, (u_1, w_2), \mathbf{v}, t_1+t_2-1} &= \begin{cases} (1-r) \cdot x_{u_2, w_2, v_2, t_2}^* & \text{if } u_1 \neq v_1, \\ x_{u_2, w_2, v_2, t_2}^* & \text{if } u_1 = v_1. \end{cases} \end{aligned} \quad (16)$$

First of all, because $d_{G_1 \square G_2}(\mathbf{u}, \mathbf{v}) = d_{G_1}(u_1, v_1) + d_{G_2}(u_2, v_2)$, it is easy to verify that (16) gives a SPFF schedule. In addition, for any distinct $\mathbf{u}, \mathbf{v} \in G_1 \square G_2$ with $u_1 \neq v_1$ and $u_2 \neq v_2$, we have

$$\begin{aligned} &\sum_{(\mathbf{u}, \mathbf{w})} x_{\mathbf{u}, \mathbf{w}, \mathbf{v}, t_1+t_2-1} \\ &= r \sum_{(u_1, w_1)} x_{u_1, w_1, v_1, t_1}^* + (1-r) \sum_{(u_2, w_2)} x_{u_2, w_2, v_2, t_2}^* \\ &= r + (1-r) \\ &= 1 \end{aligned}$$

satisfying the equality in (1). The $u_1 = v_1$ or $u_2 = v_2$ case is trivial. Because G_1 and G_2 have bandwidth optimal SPFF

schedule, by theorem 16, for any $(u_1, w_1) \in E_{G_1}$,

$$\sum_{v_1 \in N_{x_1}^{G_1}(u_1)} x_{u_1, w_1, v_1, t}^* = \frac{N_{x_1}^{G_1}}{d_1}. \quad (17)$$

Define $N_{x_1, x_2}^{G_1 \square G_2}(\mathbf{u}) = N_{x_1}^{G_1}(u_1) \times N_{x_2}^{G_2}(u_2)$, then it holds that

$$\begin{aligned} N_x^{G_1 \square G_2}(\mathbf{u}) &= \bigcup_{x_1=0}^x N_{x_1, x-x_1}^{G_1 \square G_2}(\mathbf{u}) \\ &= N_{x_1}^{G_1}(u_1) \times \{u_2\} \cup \{u_1\} \times N_{x_2}^{G_2}(u_2) \cup \bigcup_{x_1=1}^{x-1} N_{x_1, x-x_1}^{G_1 \square G_2}(\mathbf{u}). \end{aligned}$$

Thus, (17) gives

$$\sum_{\mathbf{v} \in N_x^{G_1 \square G_2}(\mathbf{u})} x_{\mathbf{u}, (w_1, u_2), \mathbf{v}, t} = \frac{N_x^{G_1}}{d_1} + r \sum_{x_1=1}^{x-1} \frac{N_{x_1}^{G_1} N_{x-x_1}^{G_2}}{d_1}. \quad (18)$$

for any $(\mathbf{u}, (w_1, u_2)) \in E_{G_1 \square G_2}$ and $t = D(G_1 \square G_2) + 1 - x$. For G_2 , one can similarly get

$$\sum_{\mathbf{v} \in N_x^{G_1 \square G_2}(\mathbf{u})} x_{\mathbf{u}, (u_1, w_2), \mathbf{v}, t} = \frac{N_x^{G_2}}{d_2} + (1-r) \sum_{x_2=1}^{x-1} \frac{N_{x-x_2}^{G_1} N_{x_2}^{G_2}}{d_2}. \quad (19)$$

The value of r is the solution to (18) = (19):

$$\frac{N_x^{G_1}}{d_1} + r \sum_{x_1=1}^{x-1} \frac{N_{x_1}^{G_1} N_{x-x_1}^{G_2}}{d_1} = \frac{N_x^{G_2}}{d_2} + (1-r) \sum_{x_2=1}^{x-1} \frac{N_{x-x_2}^{G_1} N_{x_2}^{G_2}}{d_2}.$$

To see there is always a solution $r \in [0, 1]$, we have $N_x^{G_1} \leq d_1 \cdot N_{x-1}^{G_1}$ and $N_x^{G_2} \leq d_2 \cdot N_{x-1}^{G_2}$, so

$$\begin{aligned} \frac{N_x^{G_1}}{d_1} - \frac{N_x^{G_2}}{d_2} &\leq \frac{N_x^{G_1}}{d_1} \leq N_{x-1}^{G_1} \leq \sum_{x_2=1}^{x-1} \frac{N_{x-x_2}^{G_1} N_{x_2}^{G_2}}{d_2}, \\ \frac{N_x^{G_2}}{d_2} - \frac{N_x^{G_1}}{d_1} &\leq \frac{N_x^{G_2}}{d_2} \leq N_{x-1}^{G_2} \leq \sum_{x_1=1}^{x-1} \frac{N_{x_1}^{G_1} N_{x-x_1}^{G_2}}{d_1}. \end{aligned}$$

Note that $a+rb = c+(1-r)d$ always have a solution $r \in [0, 1]$ if $a-c \leq d$ and $c-a \leq b$. With (18) = (19), by theorem 16, we have constructed a bandwidth optimal solution of (1) on $G_1 \square G_2$. The theorem trivially follows by induction. □

E SPFF Schedule

DEFINITION 6 (SHORTEST-PATH-FARTHEST-FIRST (SPFF) SCHEDULE). *A reduce-scatter schedule A on G is an SPFF schedule if A satisfies: $((v, C), (u, w), t) \in A$ if and only if $d(u, v) = d(w, v) + 1 = D(G) + 1 - t$, where $D(G)$ is graph G 's diameter.*

THEOREM 15. *If A is a SPFF schedule for G , then $T_L(A) = \alpha D(G)$.*

THEOREM 16. *Suppose (G, A) is a reduce-scatter SPFF schedule. (G, A) is bandwidth optimal if and only if:*

- (1) *There exists a sequence $N_1, N_2, \dots, N_{D(G)}$ such that for any $x \in \mathbb{N}$ and $u \in V_G$, $|N_x(u)| = N_x$, where $N_x(u) = \{v \in V_G \mid d(u, v) = x\}$.*
- (2) $\sum_{((v,C),(u,w)) \in A_t} |C| = \frac{M}{N} |N_x(u)|/d = \frac{M}{N} N_x/d$ for any $(u, w) \in E_G$ where $x = D(G) + 1 - t$.

PROOF. At comm step t , each vertex needs to send out the shards of vertices in $N_x(u)$ with $x = D(G) + 1 - t$. By (1) of theorem 5, each out edge of vertex u is sending equal amount of data, so each out edge sends out $\frac{M}{N} |N_x(u)|/d$. In addition, (1) of theorem 5 also forces every edge in G sending equal amount of data at any given comm step, so $\frac{M}{N} |N_x(u)|/d = \frac{M}{N} |N_x(v)|/d$ for all $u, v \in V_G$. Thus, we have shown the theorem as desired. \square

THEOREM 17. *There exists a bandwidth optimal SPFF schedule for undirected graph G if there exist constants N_x, a_x, b_x for all distance x such that:*

- (1) $N_x = |N_x(u)|$ for any $u \in V_G$;
- (2) $a_x = |N_x(u) \cap N_{x-1}(w)|$ for any $u \in V_G$ and $w \in N(u)$;
- (3) $b_x = |N(u) \cap N_{x-1}(v)|$ for any $u \in V_G$ and $v \in N_x(u)$.

PROOF. (1) trivially satisfies (1) of theorem 16. As for (2) of theorem 16, first of all, it is easy to see that $N_x = da_x/b_x$. At comm step t , suppose $x = D(G) + 1 - t$. Consider a SPFF schedule such that for any $u, v, w \in V_G$ with $d(u, v) = d(w, v) + 1 = x$, node u sends $1/b_x$ of v 's shard to w . Thus, $\sum_{((v,C),(u,w)) \in A_t} |C| = \frac{M}{N} a_x/b_x = \frac{M}{N} N_x/d$. \square

THEOREM 18. *A schedule A for G is a reduce-scatter SPFF schedule if and only if:*

- (1) $((v, C), (u, w), t) \in A$ if and only if $d(u, v) = d(w, v) + 1 = D(G) + 1 - t$;
- (2) *For any distinct $u, v \in V_G$, the collection of chunks $E_v = \{C \mid ((v, C), (u, w), t) \in A\}$ satisfies $S = \bigcup_{C \in E_v} C$. This condition requires that for every node v , the entire shard destined at the node reaches v .*

PROOF. Let v_0, v_k be arbitrary two distinct vertices in V_G with $d(v_0, v_k) = k$. For any $x \in S$, we want to show that there exists a shortest path taking x from v_0 to v_k . At comm step $D(G) + 1 - k$, (1) and (2) guarantee that there exists $v_1 \in N^+(v_0)$ and $((v_k, C_1), (v_0, v_1), D(G) + 1 - k) \in A$ such that $d(v_1, v_k) = k - 1$ and $x \in C_1$. At comm step $D(G) + 2 - k$, similarly, it is guaranteed that there exists $v_2 \in N^+(v_1)$ and $((v_k, C_2), (v_1, v_2), D(G) + 2 - k) \in A$ such that $d(v_2, v_k) = k - 2$ and $x \in C_2$. Thus, we have a sequence of tuples in A :

$$\begin{aligned} & ((v_k, C_1), (v_0, v_1), D(G) + 1 - k), \\ & ((v_k, C_2), (v_1, v_2), D(G) + 2 - k), \\ & \quad \vdots \\ & ((v_k, C_k), (v_{k-1}, v_k), D(G)), \end{aligned}$$

where $x \in C_1 \cap C_2 \cap \dots \cap C_k$ as desired. In the other direction, if (1) fails, then A is not a SPFF schedule; if (2) fails, then A is not a reduce-scatter schedule. \square

THEOREM 19. *Given any topology G , linear program (1) gives the optimal SPFF schedule of G .*

PROOF. All SPFF schedule on a given topology G has the same T_L . Thus, the one with optimal T_B is the optimal SPFF schedule of G . \square

The SPFF optimization problem is equivalent to a job scheduling problem. Suppose we have a set of jobs (destination nodes) $\{j_1, j_2, \dots, j_m\}$ and a set of processors (neighbors) $\{p_1, p_2, \dots, p_d\}$. There exist a map f from any job to a set of processors that j_i can only be processed by the processors in $f(j_i)$ (neighbors on shortest paths to j_i). The problem is how to schedule these jobs to processors so that workloads are balanced across all processors. Note that jobs can be arbitrarily divided into subjobs to run on processors in parallel.

THEOREM 20. *The workload can be balanced if and only if there exist no $J \subseteq \{j_1, j_2, \dots, j_m\}$ such that*

$$\frac{|J|}{|\bigcup_{j \in J} f(j)|} > \frac{m}{d}.$$

PROOF. If such a subset J exists, then it is trivial to see that the workload cannot be balanced. For the other direction, suppose no such subset J exists. Let S be any unbalanced schedule such that $S(j_a, p_b) \in [0, 1]$ is equal to the percentage of job j_a scheduled on processor p_b . We will transform schedule S to a balanced schedule.

Let E_0 be the set of processors that their workloads are above average m/d , i.e., $E_0 = \{p_b \mid \sum_a S(j_a, p_b) > m/d\}$. Let F_0 be the set of jobs that have been scheduled on any processor in E_0 , i.e., $F_0 = \{j_a \mid \exists p_b \in E_0 : S(j_a, p_b) > 0\}$. We want to find a job $j_0 \in F_0$ and $p_1 \in f(j_0) \setminus E_0$ such that we can decrease $S(j_0, p_0)$ and increase $S(j_0, p_1)$. Note that such j_0, p_1 must exist; otherwise, set F_0 is the set J mentioned above. There are two cases for such j_0, p_1 :

- If p_1 has workload less than average, i.e., $\sum_i S(j_i, p_1) < m/d$, then we can schedule part of j_0 from p_0 to p_1 to make the schedule more balanced.
- If p_1 has workload equal to average, i.e., $\sum_{j_i} S(j_i, p_1) = m/d$, then we define E_1, F_1 such that $E_1 = E_0 \cup \{p_1\}$ and $F_1 = \{j_a \mid \exists p_b \in E_1 : S(j_a, p_b) > 0\}$. We then find a job $j_1 \in F_1$ and $p_2 \in f(j_1) \setminus E_1$ such that we can decrease $S(j_1, p_1)$ and increase $S(j_1, p_2)$. Again, such j_1, p_2 must exist; otherwise, F_1 is the set J .

We can repeat the above steps, and we assert there will be a j_k, p_{k+1} that falls into the first case. If not, there will be an E_h

that includes all processors with workload equal to or greater than the average m/d , and F_h will be the set J . Thus, there will exist j_0, j_1, \dots, j_k and corresponding p_0, p_1, \dots, p_{k+1} that $p_i, p_{i+1} \in f(j_i)$, $\sum_a S(j_a, p_0) > m/d$, $\sum_a S(j_a, p_{k+1}) < m/d$, and $\sum_a S(j_a, p_i) = m/d$ for $i = 1, \dots, k$. Thus, we can continuously decrease $S(j_i, p_i)$ and increase $S(j_i, p_{i+1})$ by a same amount such that the workloads of p_1, \dots, p_k remain the same, but part of the workload of p_0 has been transferred to p_{k+1} . Thus, the schedule becomes more balanced. Since schedule S is arbitrary, we have proved the theorem. \square

E.1 Chunked SPFF Schedule

The SPFF LP (1) makes an unrealistic assumption that chunks can be divided infinitesimally. In practice, the percentages $x_{u,w,v,t}$ s are usually solved to be rational numbers. We can divide each shard into number of chunks equal to the LCM of $x_{u,w,v,t}$ s' denominators so that each $x_{u,w,v,t}$ is some integer number of chunks. However, there exists the case that each shard of the model may only be divided up to P chunks (i.e., the whole model M can only be divided up to PN chunks). In such a case, the following theorem shows that we can approximate the optimal SPFF schedule in polynomial time.

THEOREM 21. *Suppose each shard of the model can only be divided up to P chunks. Given a topology G , let T_B^{OPT} be the optimal bandwidth runtime of reduce-scatter SPFF schedule. Then, one can compute a SPFF schedule with bandwidth runtime $T_B \leq T_B^{OPT} + \frac{M}{B} \cdot \frac{d(d^{D(G)}-1)}{(d-1)PN}$ in polynomial time. In addition, if G is Moore optimal, then $T_B \leq T_B^{OPT} + \frac{M}{B} \cdot \frac{d}{P}$.*

PROOF. Consider the following integer program:

$$\begin{aligned} & \text{minimize} && W_{u,t} \\ & \text{subject to} && \sum_v y_{u,w,v,t} \leq W_{u,t}, \quad \forall (u, w) \in E_G \\ & && \sum_w y_{u,w,v,t} = P, \quad \forall v \in N_{D(G)+1-t}(u) \\ & && y_{u,w,v,t} \in \{0, 1, \dots, P\}, \quad \forall w, v. \end{aligned} \tag{20}$$

Compared with (1), one can easily see that the optimal solution of (20) gives the optimal reduce-scatter SPFF schedule when each shard of the model can only be divided up to P chunks. One can also easily solve the LP relaxation of (20) in polynomial time. Suppose the LP relaxation gives a schedule with bandwidth runtime T_B^{LP} , then we have $T_B^{LP} \leq T_B^{OPT}$.

Consider the solution to (20) obtained by rounding the optimal solution of LP relaxation. Let $y_{u,w,v,t}$ s be the rounded solution. At comm step t , there are at most $d^{D(G)-t}$ number of vs whose shortest path from u passes a given edge (u, w) . It follows that

$$\sum_v y_{u,w,v,t} < \sum_v 1 + y_{u,w,v,t}^{LP} \leq d^{D(G)-t} + \sum_v y_{u,w,v,t}^{LP}.$$

Thus, we have $W_{u,t} \leq W_{u,t}^{LP} + d^{D(G)-t}$. By (2),

$$\begin{aligned} T_B - T_B^{OPT} &\leq T_B - T_B^{LP} \\ &\leq \frac{M/N}{B/d} \cdot \frac{1}{P} \sum_{t=1}^{D(G)} d^{D(G)-t} = \frac{M}{B} \cdot \frac{d(d^{D(G)}-1)}{(d-1)PN}. \end{aligned}$$

Note that we need to divide (2) by P , because $y_{u,w,v,t} \in [0, P]$ in (20) while $x_{u,w,v,t} \in [0, 1]$ in (1). If G is Moore optimal (i.e. $N > M_{d,D(G)-1}$), it follows that

$$T_B - T_B^{OPT} < \frac{M}{B} \cdot \frac{d(d^{D(G)}-1)}{(d-1)PM_{d,D(G)-1}} = \frac{M}{B} \cdot \frac{d}{P}.$$

\square

The cost $\frac{M}{B} \cdot \frac{d}{P}$ is negligible since P can easily be hundreds or even thousands while d is usually a small integer. In practice, the solution of LP (1) is in rational values, and one can derive the appropriate P that incurs no runtime sacrifice.

E.2 Heterogeneous SPFF Schedule

The SPFF LP (1) assumes a homogeneous network. It turns out that with little modification, (1) can give an LP for heterogeneous network too:

$$\begin{aligned} & \text{min} && U_{u,t} \\ & \text{s.t.} && \alpha_{u,w} + \frac{M/N}{B_{u,w}} \sum_v x_{u,w,v,t} \leq U_{u,t}, \quad \forall (u, w) \in E_G \\ & && \sum_w x_{u,w,v,t} = 1, \quad \forall v \in N_{D(G)+1-t}(u) \\ & && 0 \leq x_{u,w,v,t} \leq 1, \quad \forall w, v \end{aligned} \tag{21}$$

Here, $\alpha_{u,w}$ and $B_{u,w}$ are the node latency and bandwidth of link (u, w) . In some cases, the α of some link (u, w') is so high that $\alpha_{u,w'}$ alone dominates $U_{u,t}$ in (21) even though $\sum_v x_{u,w',v,t} = 0$. This is problematic because one should not pay $\alpha_{u,w'}$ if there is no traffic through link (u, w') . However, such a scenario can be easily detected after solving the LP (21), and one can avoid the issue by simply removing link (u, w') and solving the LP again.

E.3 Bidirectional Ring

Ring is the most common topology for allreduce. The classic schedule on ring is to let chunks go a full circle to do reduce-scatter or allgather. In a bidirectional ring, one can simply let half of the data go clockwise and the other half go counterclockwise. Such a schedule has $N-1$ comm steps and optimal bandwidth runtime. With SPFF, we discovered a new schedule on bidirectional ring that has only $\lfloor N/2 \rfloor$ number of comm steps while still being bandwidth optimal.

Take allgather as an example. In allgather, each node wants to broadcast a shard to all other nodes. When the size of the ring is odd, one can broadcast the shard clockwise and counterclockwise at the same time. Thus, the shard only needs to go a half circle instead of a full circle. The same

works when the size of the ring is even, except at the last comm step, only one node has not received the shard. To balance the workload, we can let each of the two neighbors of the node send one half of the shard. Thus, the allgather remains bandwidth optimal. The reduce-scatter schedule can be constructed by simply reversing the communications.

E.4 Generalized Kautz Graph

In §4.1, we have introduced line graph expansion as a technique to scale a base topology to arbitrarily large size. However, the resulting topology size can only be Nd^n for some positive integer n leaving large gaps in sizes. To design an algorithm for an arbitrary size, one can use the linear program (1) on generalized Kautz graph [14, 36]:

DEFINITION 14 (GENERALIZED KAUTZ GRAPH). *The $\Pi_{d,m}$ digraph has the set of integers modulo m as vertex set. Its arc set A is defined as follows:*

$$A = \{(x, y) \mid y \equiv -dx - a, 1 \leq a \leq d\}.$$

If $m = d^{n+1} + d^n$, then $\Pi_{d,m} = K(d, n)$, where $K(d, n)$ is the Kautz graph $L^n(K_{d+1})$.

The Kautz graph $L^n(K_{d+1})$ is always Moore optimal. In fact, Kautz graph is the largest known digraph in *degree/diameter problem* for any degree $d > 2$ [50]. The following theorem shows that the node latency of generalized Kautz graph satisfies $T_L \leq T_L^*(N) + 1$:

THEOREM 22. *Suppose $D(\Pi_{d,m}) = k$, then $m \geq M_{d,k-2}$.*

PROOF. From [36], we know that $k \leq \lceil \log_d m \rceil$. Then,

$$m \geq d^{k-1} \geq \frac{d^{k-1} - 1}{d - 1} = M_{d,k-2}. \quad \square$$

From figure 13, one can also see that T_B is also close to bandwidth optimality, especially at higher degrees.

E.5 Distance-Regular Graph

In graph theory, distance-regular graphs are a family of undirected graphs. We can show that there exists a bandwidth optimal SPFF schedule for any distance-regular graph, and thus LP (1) can always compute one. We borrow the definition from [12]:

DEFINITION 15 (DISTANCE-REGULAR GRAPH). *A connected graph G is distance-regular if for any vertices $x, y \in V_G$ and integers i, j , the number of vertices at distance i from x and distance j from y depends only on i, j and $d(x, y)$.*

In other words, there exists a constant $s_{i,j}^h$ for any h, i, j such that $s_{i,j}^h = |N_i(x) \cap N_j(y)|$ whenever $x, y \in V_G$ satisfy $d(x, y) = h$. Thus, theorem 17 follows with $N_x = s_{x,x}^0$, $a_x = s_{x,x-1}^1$, and $b_x = s_{1,x-1}^x$.

The significance of distance-regular graphs is not only about having bandwidth optimal schedules. Many of

distance-regular graphs have low diameters that their schedules are not only bandwidth optimal but also close to (if not exactly) node latency optimal. Table 4 gives examples of distance-regular graphs at $d = 4$. In addition, many of the base graphs mentioned in this paper are also distance-regular like complete bipartite and Hamming graphs.

E.6 Kneser Graph

Kneser graphs [44] are another family of undirected graphs with bandwidth optimal SPFF schedules. While many Kneser graphs like odd graphs are distance-regular, there are some Kneser graphs not covered by distance-regular graphs (see table 5).

DEFINITION 16 (KNESER GRAPH). *The Kneser graph $K(n, k)$ is an undirected graph with vertices being all k -element subsets of $\{1, 2, \dots, n\}$. Two vertices are joined by an edge if and only if the two corresponding subsets are disjoint.*

Note that $K(n, k)$ is disconnected when $2k \geq n$. Thus, we restrict our discussion to Kneser graphs with $2k < n$.

Let $\pi \in S_n$ be arbitrary permutation of $\{1, 2, \dots, n\}$. Consider the mapping $f_\pi : V_{K(n,k)} \rightarrow V_{K(n,k)}$ where $f_\pi(\{x_1, \dots, x_k\}) = \{\pi(x_1), \dots, \pi(x_k)\}$. It is easy to see that f_π is an automorphism of $K(n, k)$. Now, we will show that Kneser graphs also satisfy theorem 17:

PROOF. (1): This trivially follows the fact that Kneser graphs are vertex-transitive [31].

(2): Pick arbitrary $u, u' \in V_{K(n,k)}$ and $w \in N(u), w' \in N(u')$. Since $u \cap w = \emptyset$ and $u' \cap w' = \emptyset$, it is trivial to construct a permutation $\theta \in S_n$ such that $f_\theta(u) = u'$ and $f_\theta(w) = w'$. Because f_θ is an automorphism, $|N_x(u) \cap N_{x-1}(w)| = |N_x(u') \cap N_{x-1}(w')|$ for all x .

(3): Pick arbitrary $u, u' \in V_{K(n,k)}$ and $v \in N_x(u), v' \in N_x(u')$. From lemma 2 of [67], we have $|u \cap v| = |u' \cap v'|$. Thus, we can also construct an automorphism f_θ with $f_\theta(u) = u'$ and $f_\theta(v) = v'$. It follows that $|N(u) \cap N_{x-1}(v)| = |N(u') \cap N_{x-1}(v')|$. \square

E.7 Circulant Graph

Circulant graph is a well-studied topology in both graph theory and network design. Many popular network topologies like shifted ring, chordal ring, and loop network are either part of or closely related to circulant graphs. The definition of circulant graph is as followed:

DEFINITION 17. *The circulant graph $C(n, \{a_1, \dots, a_k\})$ is a bidirectional graph with vertex set $\{0, 1, \dots, n-1\}$ and each node i is adjacent to nodes $i \pm a_1, \dots, i \pm a_k \pmod{n}$.*

Note that in this paper, we only consider connected circulant graphs, and $C(n, \{a_1, \dots, a_k\})$ is connected if and only if $\gcd(n, a_1, \dots, a_k) = 1$ [46, 51]. It is easy to see that $C(n, \{a_1, \dots, a_k\})$ is an n -node $2k$ -regular topology.

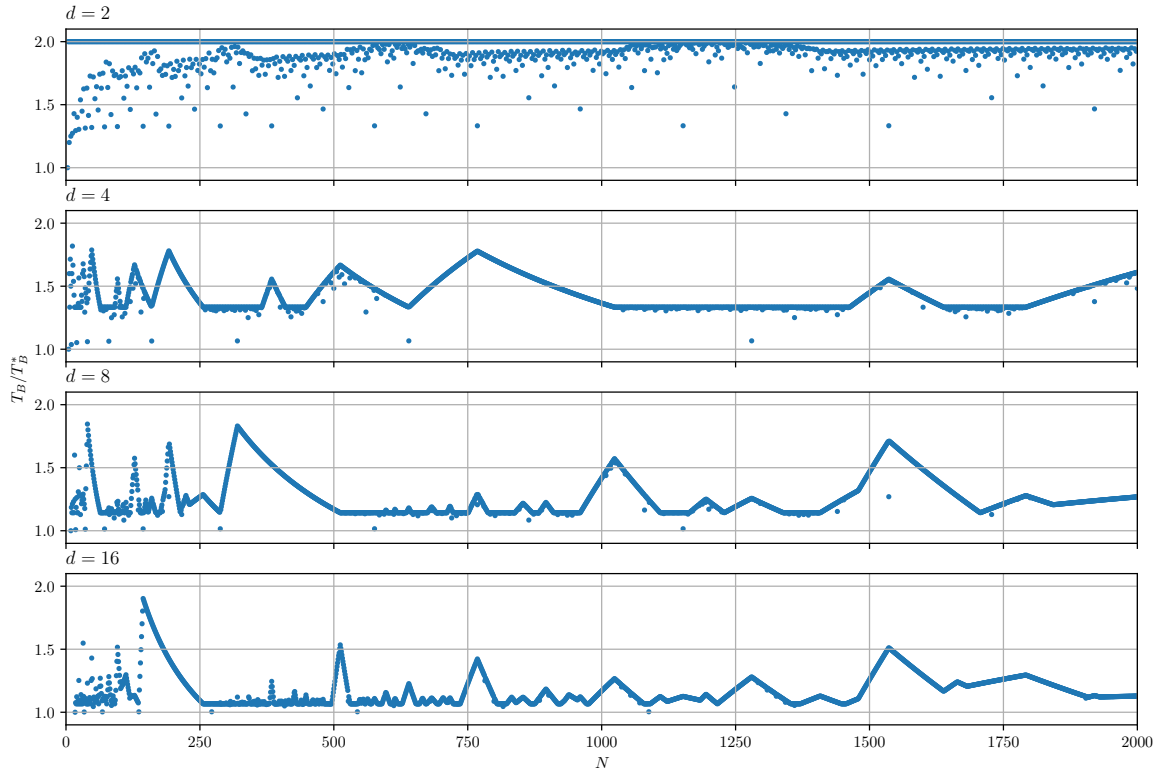


Figure 13: T_B/T_B^* of generalized Kautz graph $\Pi_{d,N}$ up to $N = 2000$. As one can see that the bandwidth runtime of $\Pi_{d,N}$ is less than or equal to $2T_B^*$ at all time for $d = 2, 4, 8, 16$. In particular, the higher the degree is, the closer T_B is to optimal. As for node latency, theorem 22 shows that $T_L \leq T_L^*(N) + 1$.

Graph Name	N	T_L	T_L^*	$T_L - T_L^*$	T_L^{**}	$T_L - T_L^{**}$
Octahedron J(4,2)	6	2	2	0	2	0
Paley graph P9 \cong H(2,3)	9	2	2	0	2	0
K5,5-I	10	3	2	1	2	1
Distance-3 graph of Heawood graph	14	3	2	1	2	1
Line graph of Petersen graph	15	3	2	1	2	1
4-cube Q4 \cong H(4,2)	16	4	2	2	2	2
Line graph of Heawood graph	21	3	2	1	3	0
Incidence graph of PG(2,3)	26	3	3	0	3	0
Incidence graph of AG(2,4) minus a parallel class	32	4	3	1	3	1
Odd graph O4	35	3	3	0	3	0
Line graph of Tutte's 8-cage	45	4	3	1	3	1
Doubled Odd Graph D(O4)	70	7	3	4	4	3
Incidence graph of GQ(3,3)	80	4	3	1	4	0
Line graph of Tutte's 12-cage	189	6	4	2	5	1
Incidence graph of GH(3,3)	728	6	5	1	6	0

Table 4: Examples of distance-regular graphs at $d = 4$ [2]. T_L^{**} is the bidirectional Moore optimality.

At later stage of our research, we found that the SPFF LP (1) seems to give bandwidth optimal schedules for all circulant graphs. In particular, we have the following conjecture:

CONJECTURE 1. *Given any connected circulant graph $C(n, \{a_1, \dots, a_k\})$, there exists a bandwidth optimal SPFF schedule.*

While we leave a complete proof or disproof of this conjecture for future work, we have proved for a special type of circulant graphs and computationally verified many. Circulant graph revolutionized our Pareto frontier of topologies since it can be constructed for every N and even d . It can provide a bandwidth optimal topology if our expansion techniques fail

	d	N	T_L	T_L^*	$T_L - T_L^*$	T_L^{**}	$T_L - T_L^{**}$
$K(5, 2) \cong O_3$	3	10	2	2	0	2	0
$K(7, 3) \cong O_4$	4	35	3	3	0	3	0
$K(9, 4) \cong O_5$	5	126	4	3	1	4	0
$K(6, 2)$	6	15	2	2	0	2	0
$K(11, 5) \cong O_6$	6	462	5	4	1	4	1
$K(13, 6) \cong O_7$	7	1716	6	4	2	4	2
$K(15, 7) \cong O_8$	8	6435	7	5	2	5	2
$K(17, 8) \cong O_9$	9	24310	8	5	3	5	3
$K(7, 2)$	10	21	2	2	0	2	0
$K(8, 3)$	10	56	2	2	0	2	0
$K(19, 9) \cong O_{10}$	10	92378	9	5	4	6	3
$K(21, 10) \cong O_{11}$	11	352716	10	6	4	6	4
$K(23, 11) \cong O_{12}$	12	1352078	11	6	5	6	5
$K(25, 12) \cong O_{13}$	13	5200300	12	6	6	7	5
$K(27, 13) \cong O_{14}$	14	20058300	13	7	6	7	6
$K(8, 2)$	15	28	2	2	0	2	0
$K(10, 4)$	15	210	3	2	1	2	1
$K(29, 14) \cong O_{15}$	15	77558760	14	7	7	7	7
$K(31, 15) \cong O_{16}$	16	300540195	15	8	7	8	7

Table 5: Connected Generalized Kneser Graphs of degree $2 \leq d \leq 16$

to produce one at some N and d . Since all circulant graphs seem to be bandwidth optimal, the question is what choices of a_1, \dots, a_k result in minimum node latency or equivalent minimum diameter at a given n . While this remains largely an open question in graph theory [51], the case of $k = 2$ has been solved in [16]:

THEOREM 23. *Given $n > 6$ and $m = \lceil (-1 + \sqrt{2n-1})/2 \rceil$, circulant graph $C(n, \{m, m+1\})$ has a diameter equal to m , which is the minimum diameter over all circulant graphs $C(n, \{a_1, a_2\})$.*

We have computationally verified such construction of degree 4 circulant graphs has bandwidth optimal SPFF schedule for all $n \leq 2000$. While we are unable to prove the bandwidth optimality of all circulant graphs with such construction, we are able to prove for a special case of it.

A commonly adopted way to analyze the $k = 2$ circulant graphs is to draw a shortest-path lattice of all vertices as in figure 14. The lattice shows how each vertex of the circulant graph can be reached from node 0 with edges $\pm a_1, \pm a_2$ through the shortest paths. For example, in figure 14a, there are three shortest paths from node 0 to 10: $0 \rightarrow 3 \rightarrow 6 \rightarrow 10$, $0 \rightarrow 3 \rightarrow 7 \rightarrow 10$, and $0 \rightarrow 4 \rightarrow 7 \rightarrow 10$. Given an node at coordinate (x, y) , its distance from node 0 is equal to $|x| + |y|$. Note that while one can continue to expand the lattice, the expansion will simply be repetitions and will not give shortest-path lattice anymore. Eventually, the expansion

will tessellate the plane with repetitions of the shortest-path lattices.⁵

As in degree/diameter problem, the problem of constructing a circulant graph with the minimum diameter given n is closely related to that of constructing a circulant graph with maximum n given a diameter. The construction in theorem 23 also generates the largest circulant graph given any diameter m at $k = 2$. The circulant graph is the largest when the shortest-path lattice is “perfect”, i.e., the lattice is a full rhombus/square and has no repetition of nodes [51, 73]. Figure 14a gives the example of a perfect shortest-path lattice, while the one in figure 14b is imperfect. We will prove that when the shortest-path lattice is perfect, the SPFF LP (1) can give a bandwidth optimal schedule.

PROOF. Because circulant graphs are vertex-transitive [46], condition (1) of theorem 16 is trivially satisfied. Now, at any comm step t , the destination nodes with which node 0 has to send out chunks form the edges of a rhombus. For example, in figure 14, node 0 has to send chunks with destinations $\{8, 7, 6, 24, 17, 18, 19, 1\}$ at comm step 2. There are two types of destination nodes:

- Node on x or y axis like $\{8, 6, 17, 19\}$. Such node has a unique shortest path from node 0, and the path passes through the out edge of node 0 on the same half axis. For example, node 6 has a unique shortest path passing through edge $(0, 3)$. The amount of data sending to such

⁵For more information on tessellation, one can refer to figure 5.8 of [46], figure 2 of [51], and figure 3 of [73].

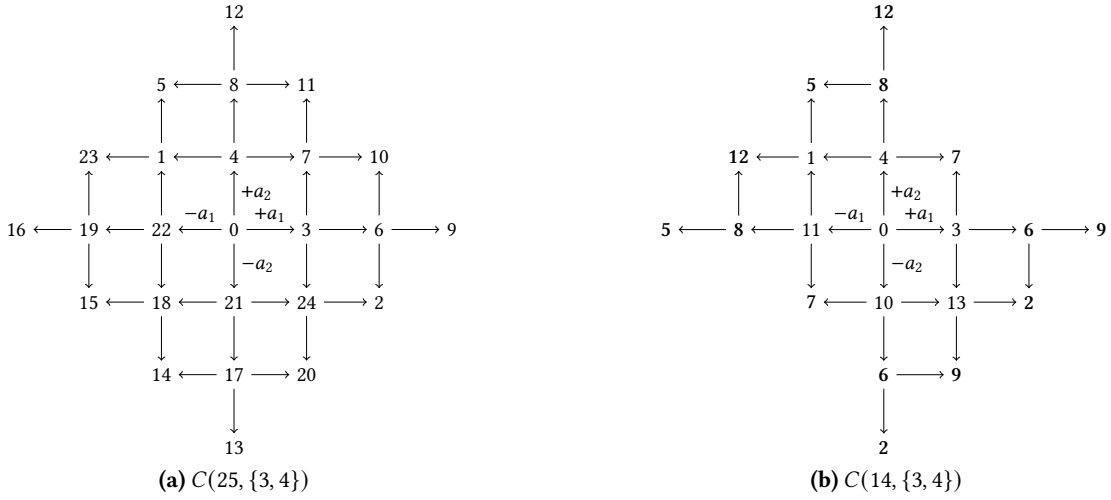


Figure 14: The shortest-path lattices of $C(25, \{3, 4\})$ and $C(14, \{3, 4\})$. While having the same $\{a_1, a_2\}$ and diameter, $C(25, \{3, 4\})$ has a perfect shortest-path lattice but $C(14, \{3, 4\})$ has not. The bolded nodes in $C(14, \{3, 4\})$ have repetition in the shortest-path lattice.

node through the corresponding link is thus equal to 1 shard, i.e., $x_{0,3,6,2} = 1$.

- Node not on any axis like $\{7, 24, 18, 1\}$. Such node has multiple shortest paths passing through exactly two of the out edges of node 0. For example, node 7 can be reached by shortest paths passing through link $(0, 3)$ or $(0, 4)$. The amount of data sending through each of the two links is thus equal to $1/2$ shard, i.e., $x_{0,3,7,2} = x_{0,4,7,2} = 1/2$.

At comm step t , suppose $h = D(G) + 1 - t$ where G is constructed with a perfect shortest-path lattice, then $N_h = 4h$. The traffic through each out edge of node 0 is $\frac{M}{N} [1 + 2(h-1) \cdot \frac{1}{2}] = \frac{M}{N} \cdot h = \frac{M}{N} N_h / d$. Again, because of the vertex transitivity of circulant graphs, the same reasoning can be applied to the shortest-path lattice originating at any node. Thus, condition (2) of theorem 16 also holds. \square

F Cartesian Power Graphs

We list several examples of Cartesian power graphs, and investigate their collective performance under the algorithm detailed in Section 4.3.

F.1 Multidimensional directional torus

The n -dimensional directed torus $M_{\ell,n}$ is a n -way Cartesian product graph with each graph being a unidirectional ring on ℓ nodes. As a result, nodes u in $M_{\ell,n}$ can be indexed by an n -tuple, (u_1, u_2, \dots, u_n) , with $0 \leq u_j < \ell$ and $N = \ell^n$. The nodes indexed by $(u_1, \dots, u_{j-1}, k, u_{j+1}, \dots, u_n)$, $0 \leq k < \ell$ together form a unidirectional ring, i.e., varying just one component of the index tuple produces a ring subgraph. This observation generalizes to any Cartesian power graph. That is, given an arbitrary vertex $\mathbf{u} \in V_G^n = V_{G^{\square n}}$, the subgraph induced by vertices $\{(\mathbf{u}[1 : i-1], v_i, \mathbf{u}[i+1 : n]) \mid v_i \in V_G\}$ is isomorphic to G , where $(\mathbf{u}[1 : i-1], v_i, \mathbf{u}[i+1 : n]) =$

$(u_1, \dots, u_{i-1}, v_i, u_{i+1}, \dots, u_n)$. Let $H_{\mathbf{u},i}$ be such a subgraph, then there are $n|V_G|^{n-1}$ such subgraphs all isomorphic to G . In addition, all such subgraphs have disjoint edge sets, so there is no congestion if we run allgather on these subgraphs simultaneously. As shown in Figure 15, each node \mathbf{u} in the torus $M_{\ell,2}$ belongs to two subgraphs – $H_{\mathbf{u},1}$ and $H_{\mathbf{u},2}$, the horizontal and vertical ring containing node \mathbf{u} respectively. Each subgraph is isomorphic to the ring on ℓ nodes.

We now describe how to construct schedules for Cartesian power graphs by using the allgather operation on a 2-dimensional directed torus as an example. We consider two messages schedules: the schedule $A^{(1)}$ corresponds to allgather performed along the horizontal ring and then along the vertical ring, while the schedule $A^{(2)}$ corresponds to allgather performed in the opposite order. Each node $\mathbf{u} = (u, v)$ in the torus divides the data into 2 subshards S'_u, S''_u and uses the two schedules on the two subshards. In accordance to schedule $A^{(1)}$, the first subshard S'_u gets allgathered along with the corresponding subshards of other nodes in the horizontal ring $H_{\mathbf{u},1}$ first, and then along vertical rings $\{H_{(u,w),2}, w = 1, \dots, \ell\}$; while following schedule $A^{(2)}$, subshard S''_u gets allgathered along the corresponding subshards of nodes in the vertical ring $H_{\mathbf{u},2}$ and then along horizontal rings $\{H_{(w,v),1}, w = 1, \dots, \ell\}$. The combined schedule, where $A^{(1)}$ and $A^{(2)}$ are performed *simultaneously*, will be bandwidth optimal since all the links are fully utilized. The node latency of the collective would be $2(\ell - 1)$.

The above schedule generalizes to arbitrary Cartesian product graphs. Consider the following *allgather* schedule, denoted as $A^{(i)}$: For a given i ($1 \leq i \leq n$), do allgather on subgraphs in order $i, i+1, \dots, n, 1, \dots, i-1$. There are n such schedules. We then consider the cumulative schedule $A_{G^{\square n}}$ that divides each shard into n equal-size subshards and lets

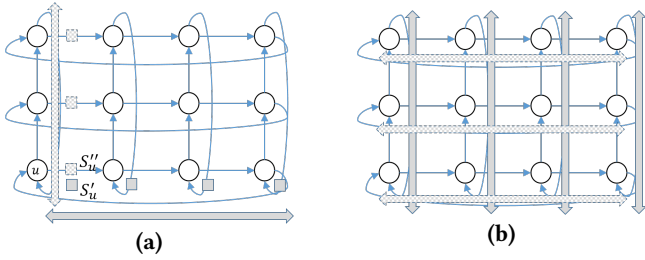


Figure 15: (a) First step where the first subshard gets allgathered horizontally and the second subshard gets allgathered vertically; (b) Second step where the subshard allgathered horizontally in the earlier step gets allgathered vertically and vice versa.

Topologies	N	Degree	Node Latency	Asymptotic Latency cost
$d = 2, n = 3$ 3 × 3 torus	9	2	4	1
$d = 2, n = 4$ 4 × 4 torus	16	2	6	2
$d = 2, n = 5$ 5 × 5 torus	25	2	8	4
$d = 3, n = 2$ 3-d hypercube	8	3	3	1
$d = 3, n = 3$ 3 × 3 × 3 torus	27	3	6	3
$d = 4, n = 2$ 4-d hypercube	16	4	4	2
$d = 4, n = 3$ 3 × 3 × 3 × 3 torus	81	4	8	5

Table 6: Node latency cost of various Cartesian product graphs with respect to Moore’s bound

$A^{(i)}$ perform allgather on all the i th subshards of nodes. Observe that by performing $A^{(1)}, \dots, A^{(n)}$ simultaneously, all edges are utilized, and there is no congestion between any two schedules of $A^{(1)}, \dots, A^{(n)}$, because there is exactly one $A^{(i)}$ performing allgather on any $H_{u,i}$ at anytime.

With the torus $M_{\ell,n}$ as a base graph, the line transformation will have a BW delay cost of $\Phi\left(\frac{1}{(n-1)N}\right)$. Note that for any fixed degree d , we can get base graphs arbitrarily close to BW delay optimality. The node latency cost will be approximately $d(\ell - 1) - d \log_d \ell$ with respect to the Moore’s lower bound.

F.2 Hypercubes

n -hypercube is a special case of n -dimensional torus with 2 nodes in each dimension connected by a bidirectional edge. The BW optimal algorithm in each dimension, $A^{(i)}$, exchanges the model between the two nodes in the same dimension. Following previous results, the product collective will be BW optimal and will have node latency n units.

F.3 Hamming graphs

Hamming graphs $H(n, q)$ is the Cartesian product of n complete graphs K_q . The BW optimal algorithm in each dimension performs the full torus collective. Following Corollary 9, the product collective will be BW optimal as well with node latency n units.

F.4 Cycle-mesh graphs

Since the multidimensional directed torus topology described in F.1 takes an n -way cartesian product of rings of length ℓ , it has number of nodes scaling as $N = \ell^n$. We present a construction that loosens this restriction on N and produces graph that has $N = r \times c$ where $r \neq c$. This offers more degrees of freedom in the graph expansion process since this process allows the generation of a base graph on any N that is factorizable into a product of two non-trivial factors. First, we observe that a standard rectangular (r, c) wraparound mesh where $r \neq c$ may not lead to ring-based bandwidth optimal schedules. This is because if $r < c$, the ring reduce/gather in the c dimension takes more comm steps than the ring reduce/gather in the r dimension, thus leading to suboptimal bandwidth-delay performance. We avoid this by following a different construction.

Suppose we want to build a bandwidth optimal graph on $N = 15$ nodes with good node latency properties. Observe that $N = 3 \times 5$ (thus $r = 3, c = 5$). We group the set of $N = 15$ nodes into $r = 3$ groups of $c = 5$. For such factorizable N , it is always possible to cover the set of N nodes by a union of r disjoint rings of length c in two different ways. In this example, the first way is to just put the first $c = 5$ nodes into the first ring $\{1, 2, 3, 4, 5\}$, the second set of 5 into the second ring $\{6, 7, 8, 9, 10\}$, and the third set of 5 in the third ring $\{11, 12, 13, 14, 15\}$, etc. The second way is to skip the node indices in each ring by $r = 3$, e.g., the first ring will be $\{1, 4, 7, 10, 13\}$, the second will be $\{2, 5, 8, 11, 14\}$ and the third ring will be $\{3, 6, 9, 12, 15\}$. Now we have $r = 3$ sets of $c = 5$ -rings in two different dimensions, and hence we can do ring reduce/gather with equal number of comm steps ($c = 5$) in each dimension. Following the methods used for constructing schedules for n step cartesian product of rings from individual steps, we can construct a bandwidth optimal schedule for this $N = r \times c$ node graph.

Note that to be able to construct ring reduce/gather schedules, a necessary property that must hold is that for each ring R_i in the first dimension, the set of orthogonal rings (i.e., rings in the second dimension) passing through each of the nodes in R_i must cover the entire vertex space; otherwise the two-step ring reduce/gather procedure will not reach all nodes in the graph. Our construction satisfies this property.

Since the length of all the rings is equal to $\max(r, c)$, the reduce/gather node latency for the 2-step process = $2 \max(r -$

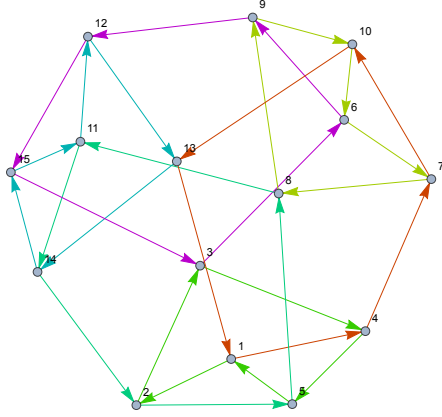


Figure 16: $N = r \times c$ node cycle mesh ($r = 3, c = 5$)

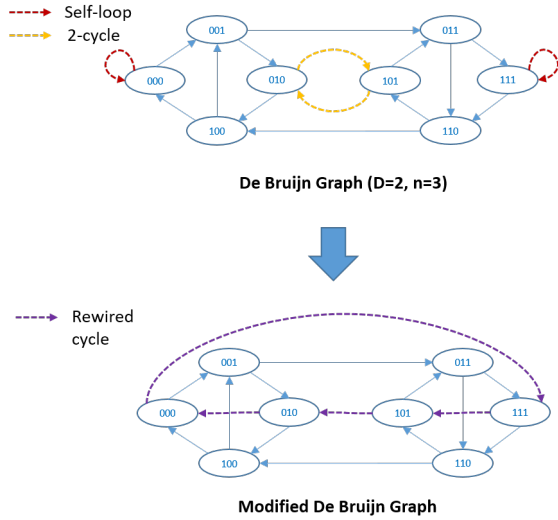


Figure 17: Modification of De-Bruijn graph shown for $d = 2, n = 3$

$1, c - 1$). Thus for factorizations of N where r, c are the closest in value to \sqrt{N} , we can achieve low-node-latency bandwidth optimal schedules. Figure 16 shows the bandwidth optimal topology for $N = 15$ with node latency 8. This is not too far off from the 16 node perfect square wraparound mesh with node latency equal to 6.

G Modifying the De-Bruijn graph

An n -dimensional d -symbol De-Bruijn graph $G = (V, E)$ has d self loops at the following nodes $\{(s, s, \dots, s), s = 0, 1, \dots, d-1\}$, and $\frac{d(d-1)}{2}$ number of 2-cycles involving nodes of the form $\{(s_1, s_2, \dots), s_1 \neq s_2\}$. We propose modifying the De-Bruijn graph where the self loops and 2-cycles are removed and a single long cycle is constructed. Note that this process does not violate the degree regularity of the graph.

Let the nodes involved in self loops and 2-cycles be denoted as V' . Note that $|V'| = d^2$. A valid modification that introduces a long cycle given by the edge set $E' \subset V' \times V'$

must satisfy the following: For every edge $e = (u, v) \in E'$, both e and $e' = (v, u)$ must not appear in the De-Bruijn graph unless they belong to a 2-cycle. This ensures that a multiedge or a 2-cycle does not get formed due to the modification.

We construct a symmetric directed graph G' on the vertex set V' that only contains symmetric directed edges that do not appear in the graph G (in either direction) unless they are 2-cycles in G . The problem of finding a valid modification boils down to finding an undirected Hamiltonian cycle in the symmetric directed graph G' viewed as an undirected graph.

Any node u in G' which participated in either a self loop or a 2-cycle in G must have degree at least $d^2 - 2(d-1) - 1$. This lower bound is obtained by considering the worst case scenario where all the outdegrees and indegrees of u , not considering the self loop or the 2-cycle, were to lie in V' . Using Ore's theorem [72] which states that a Hamiltonian circuit exists if every node of a graph $G'' = (V'', E'')$ has degree at least $|V''|/2$, we obtain that for $d \geq 4$ we will always be able to perform a modification. We use efficient algorithms for finding Hamiltonian cycles in dense graphs for the purpose of making such modifications [27]. For $d = 2, 3$, only a small number of nodes are involved in the rewiring process, and thereby brute force approaches for finding Hamiltonian cycles are sufficient. Figure 17 shows the modification process on a 8 node binary De-Bruijn graph.

H Synthetic topology generation

H.1 Notation

N	Number of nodes
V	Node set = $\{0, 1, \dots, V - 1\}$
d	Desired out-degree and in-degree of each node
C	Set of commodities. These are the flows $\{s \rightarrow t, \forall s, t : s \neq t, s, t \in V\}$
Cap	Link capacity (equal for all links in what follows)
x_{ij}	Indicator variable denoting if link $i \rightarrow j$ should exist. $\forall i, j \in V, x_{ij} \in \{0, 1\}$
f_{ijc}	Flow variable pertaining to commodity c along link $i \rightarrow j$. $\forall i, j \in V, c \in C : 0 \leq f_{ijc} \leq Cap, f_{ijc} \in \mathbb{R}$
k	Demand variable for each commodity (considered equal from each source to target), $k \in \mathbb{R}$

H.2 Mixed Integer Quadratic Programming

The quadratic program optimizes the decision of laying down the links between each pair of nodes while adhering to the degree constraint, the flow conservation constraints, such that the per-node demand (throughput) is maximized. A uniform throughput maximizing solution that yields optimal rates at each node also corresponds to a minimum bandwidth-delay

solution. Note that although we do not attempt to explicitly minimize the node-latency metric, we find that this optimization formulation tends to find low diameter topologies due to the d -regularity requirement and the all-to-all nature of the traffic load. In other words, a high-diameter topology is unlikely to be the one that has the highest throughput since all nodes are supposed to communicate with every other node.

$$\begin{aligned}
& \max k \\
& \text{subject to constraints:} \\
& \forall (i, j) \in V \times V : \sum_{c \in C} x_{ij} f_{ijc} \leq \text{Cap} \\
& \forall j \in V : \sum_i x_{ij} = d \\
& \forall j \in V : \sum_i x_{ji} = d \\
& \forall c \in C, \forall j \in V, j \neq s(c), j \neq t(c) : \sum_i x_{ij} f_{ijc} = \sum_i x_{ji} f_{jic} \\
& \forall c \in C, j = s(c) : \sum_i x_{ij} f_{ijc} = k \\
& \forall c \in C, j = t(c) : \sum_i x_{ij} f_{ijc} = k
\end{aligned}$$

The first constraint ensures that the total amount of traffic flowing through each link (i, j) (summed over all commodities) does not exceed the link's capacity. The second and the third constraints enforce the out-degree and in-degree requirements. The fourth constraint ensures per-commodity flow conservation at each node j that is neither the source nor the target for that commodity. The fifth and the sixth constraints ensure that each source and sink of a commodity, respectively, *sources* and *sinks* are given (equal) amount of traffic, k , which is the quantity that needs to be maximized.

H.3 Linearization of the Quadratic Program

Mixed integer quadratic programs (MIQP) are prohibitively expensive to solve even using state-of-the-art solvers like Gurobi, especially if the constraints are quadratic as well, which is the case above. However, we exploit some special structure in the problem that helps us *linearize* it as follows.

When encountering the product $x \cdot f$, one can introduce a real-valued variable $z = x \cdot f$. If x is binary-valued and f is real valued and has lower and upper bounds, i.e., $L \leq f \leq U$, the following constraints can be added to linearize the problem while preserving the structure of the solution:

$$\begin{aligned}
z &\leq Ux \\
z &\geq Lx \\
z &\leq f - L(1 - x) \\
z &\geq f - U(1 - x)
\end{aligned}$$

Applying the above transformation to the MIQP, the equivalent Mixed Integer Linear Program (MILP) is as follows:

$$\begin{aligned}
& \max k \\
& \text{subject to constraints:} \\
& \forall (i, j) \in V \times V : \sum_{c \in C} z_{ijc} \leq \text{Cap} \\
& \forall j \in V : \sum_i x_{ij} = d \\
& \forall j \in V : \sum_i x_{ji} = d \\
& \forall c \in C, \forall j \in V, j \neq s(c), j \neq t(c) : \sum_i z_{ijc} = \sum_i z_{jic} \\
& \forall c \in C, j = s(c) : \sum_i z_{ijc} = k \\
& \forall c \in C, j = t(c) : \sum_i z_{ijc} = k \\
& \forall (i, j) \in V \times V, c \in C : z_{ijc} \leq \text{Cap} \cdot x_{ij} \\
& \forall (i, j) \in V \times V, c \in C : z_{ijc} \geq 0 \\
& \forall (i, j) \in V \times V, c \in C : z_{ijc} \leq f_{ijc} \\
& \forall (i, j) \in V \times V, c \in C : z_{ijc} \geq f_{ijc} - \text{Cap} \cdot (1 - x_{ij})
\end{aligned}$$

Although MILPs are also computationally intractable in general, it is tractable for small values of N . This allows us to produce interesting base graphs that can be *expanded* using the techniques proposed in this paper, while preserving the bandwidth and node latency optimality properties of the synthesized base graphs.

I Pareto-Efficiency Analysis

There could exist multiple Pareto-efficient topologies at given N and d . For different α and M/B , the Pareto-efficient topology with minimum total runtime is also different. To see how N affects the optimality of topologies, we generate Pareto-efficient topologies at $d = 4$ for N up to 2000 and pick the best one based on α and M/B .

Figure 18 shows two examples of such analyses. At $M = 1\text{MB}$, node latency optimality is more important than bandwidth optimality. Thus, we see GenKautz graphs as being the best fallback option for all N . On the contrary, at $M = 100\text{MB}$, bandwidth optimality becomes the dominant factor and thus circulant graphs become the best fallback. Line graphs feature frequently in both settings; however, line graph expansion requires N to be divisible by some power of d , so it does not work for every N .

J Cost Model Validation

Despite the wide acceptance of α - β cost model by previous literature [18, 20, 34, 56, 58], we also did a linear regression analysis to verify the cost model on our testbed. In particular, we want to verify that (1) node latency follows $T_L = \alpha \cdot x + \epsilon$ and (2) bandwidth runtime follows $T_B = \frac{M}{B} \cdot y$, where x is the number of comm steps and b is the bandwidth factor ($y = 2 \cdot \frac{N-1}{N}$ if bandwidth optimal). ϵ is the constant latency⁶ including time costs such as GPU kernel launching. Here, we use linear regression to derive the values of α , ϵ , and $1/B$, and compute the relative errors between observed runtime and fitted runtime. We pick the allreduce runtime at 1KB as the node latency, since bandwidth runtime is negligible

⁶This part of latency is a fixed constant for all topologies and schedules, so it is omitted in earlier mathematical discussion.

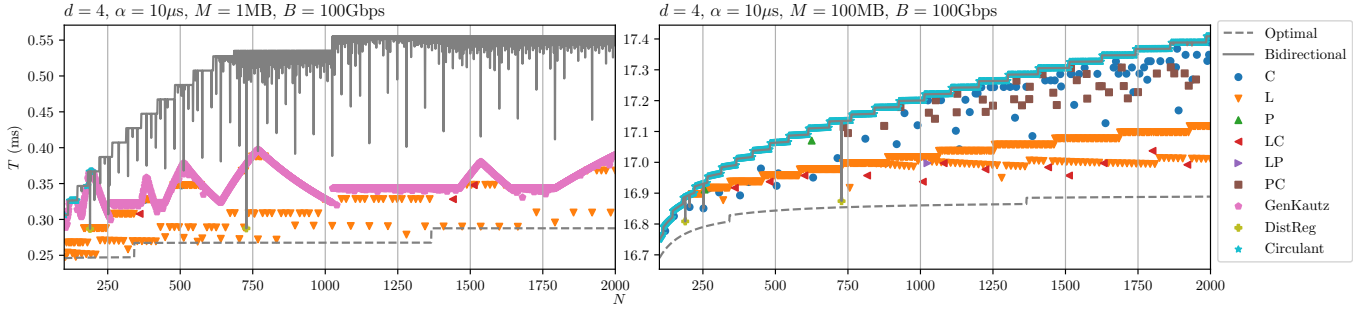
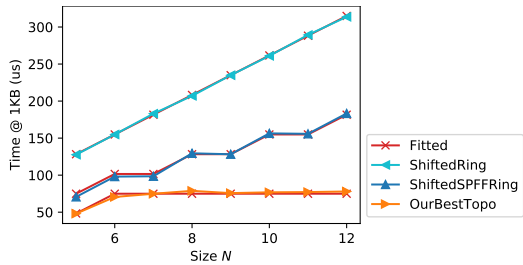
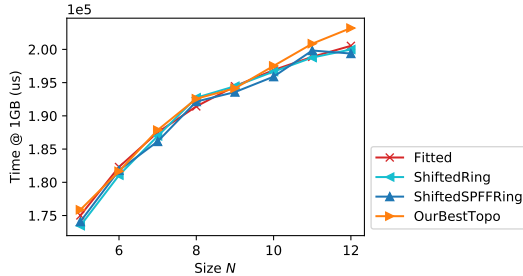


Figure 18: The minimum allreduce runtimes at different N for $d = 4$, $\alpha = 10\mu\text{s}$, and $M/B = 1\text{MB}/100\text{Gbps}$, $100\text{MB}/100\text{Gbps}$. “L”, “P”, and “C” stand for line graph, Cartesian power, and Cartesian product (of different graphs) respectively. For example, “LC” means the runtime is achieved by a topology whose construction involves line graph expansion and Cartesian product. “GenKautz”, “DistReg”, and “Circulant” stand for generalized Kautz graph (§E.4), distance regular graph (§E.5), and circulant graph (§E.7) respectively.



(a) Node latency T_L (Relative error: avg 1.71%, max 6.21%)



(b) Bandwidth runtime T_B (Relative error: avg 0.47%, max 1.32%)

Figure 19: Linear regression results.

at such a small M . Similarly, we pick runtime at 1GB as the bandwidth runtime, since node latency is negligible at such a large M .

We did not include double binary tree, because it is not a strictly regular topology, and it has a different construction of allreduce (reduce+broadcast). Thus, it is expected to have a different set of values for α , ϵ , and $1/B$. We only do regression analysis on shifted ring with naive ring allreduce, shifted ring with SPFF ring allreduce, and our topologies.

Figure 19a and 19b show our results of linear regression analysis to verify our cost model. For the node latency term, through linear regression we obtain the estimates, $\alpha \approx 13.33\mu\text{s}$ and $\epsilon \approx 21.60\mu\text{s}$, with low error values (average and maximum errors of 1.71% and 6.21% respectively). As one can see from figure 19a, naive shifted ring

and shifted ring with SPFF ring allreduce have a straight and a stair-step shape of runtime growth respectively, which match the expected numbers of comm steps $2(N-1)$ and $2\lfloor N/2 \rfloor$ respectively. For the bandwidth term, we get the estimate $1/B \approx 0.0001018\mu\text{s}/\text{byte}$ or $B \approx 79\text{Gbps}$, with low error values (average and maximum errors of 0.47% and 1.32% respectively). As one can see from figure 19b, all three topologies follow the fitted curve $2\frac{1\text{GB}}{B} \cdot \frac{N-1}{N} = 2T_B^*(N)$ since they are all bandwidth optimal. However, there is a gap between $B \approx 79\text{Gbps}$ and the hardware theoretical bandwidth $4 \times 25\text{Gbps} = 100\text{Gbps}$. Besides inevitable loss of bandwidth in actual communication, the gap can also be explained by the fact that reduction cost also accounts for part of $1/B$ as discussed in §C.

K Directed to Undirected

While this paper focuses on directed topologies, many of the techniques can be conveniently applied to undirected topologies. For example, the shortest-path schedule including the linear program (1), degree expansion, and Cartesian product can all be used on undirected topologies. Although line graph expansion does not apply to undirected topologies, there is a way to convert a directed-topology schedule to undirected-topology schedule. In this section, we will show how to convert a skew-symmetric d -regular directed topology G and its reduce-scatter schedule A to a $2d$ -regular undirected topology G' and its schedule A' such that $T_L(A) = T_L(A')$ and $T_B(A) = T_B(A')$.

Let $g : V_G \rightarrow V_{G^T}$ be the isomorphism from G to G^T , then it is trivial to see that $g(A)$ is a reduce-scatter schedule for G^T . Observe that $G' = G \cup G^T$ is a $2d$ -regular undirected topology. Consider schedules A and $g(A)$ as schedules for undirected topology G' . A or $g(A)$ alone is a reduce-scatter schedule for G' . In addition, A and $g(A)$ do not congest on any edge, because $g(A)$ and A use opposite directions of edges. Thus, we can divide each shard into two halves. Let one half follow schedule A and the other half follow $g(A)$. Let such schedule be A' .

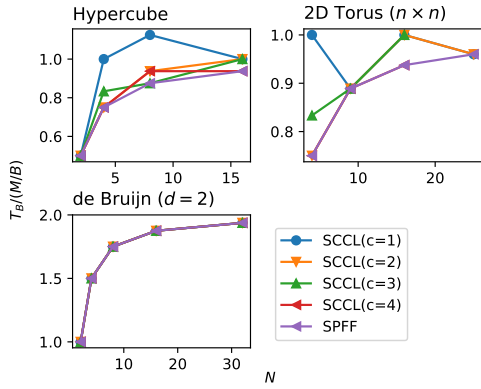


Figure 20: Comparing bandwidth performances of schedules in Figure 12. Note that both SCCL and SPFF were set to generate schedules with least number of comm steps, so SCCL schedules have the same T_L as SPFF schedules have.

It is trivial to see that $T_L(A) = T_L(A')$. As for $T_B(A) = T_B(A')$, it follows the fact that the total model size is halved for each of A and $g(A)$, but the bandwidth per edge is also halved due to the double of degree. Note that if A is bandwidth optimal, then A' is bandwidth optimal; however, A' is not necessarily node latency optimal if A is node latency optimal.

Topology	Symbol	Degree	Size	Skew-Symmetric	Bandwidth Optimal	Moore Optimal	SPFF Schedule	Self-Loop	MultiEdge
Complete	K_m	$m - 1$	m	✓	✓	✓	✓	×	×
Complete Bipartite	$K_{d,d}$	d	$2d$	✓	✓	✓	✓	×	×
Hamming	$H(n, q) = K_q^{\square n}$	$n(q - 1)$	q^n	✓	✓	$T_L = n$	✓	×	×
Kautz	$K(d, n) = L^n(K_{d+1})$	d	$d^n(d + 1)$	✓	when $n = 0$	✓	✓	×	×
Generalized Kautz	$\Pi_{d,m}$	d	$m \geq d + 1$	×	when $m = d + 1$	$T_L \leq T_L^* + 1$	✓	when $m \bmod (d + 1) \neq 0$	×
Circulant	$C(m, \{a_1, \dots, a_d\})$	d	m	✓	✓	×	✓	×	×
Directed Circulant		d	$d + 2$	✓	✓	✓	✓	×	×
Bidirectional Ring	$\text{BiRing}(d, m)$	even d	$m \geq 3$	✓	✓	$T_L = \lfloor m/2 \rfloor$	✓	×	when $d > 2$
Unidirectional Ring	$\text{UniRing}(d, m)$	d	m	✓	✓	$T_L = m - 1$	✓	×	when $d > 1$
Diamond		2	8	×	✓	✓	×	×	×
De Bruijn		d	d^n	✓	when $n \leq 1$	✓	✓	✓	×
Modified De Bruijn	$\text{DBJMod}(2, 3)$	2	8	✓	✓	$T_L = 4$	×	×	×
	$\text{DBJMod}(2, 4)$	2	16	×	✓	$T_L = 5$	×	×	×
	$\text{DBJMod}(3, 2)$	3	9	×	✓	$T_L = 3$	×	×	×
	$\text{DBJMod}(4, 2)$	4	16	×	✓	$T_L = 3$	×	×	×
Distance-Regular Graphs			✓	✓	✓	✓	✓	×	×

Table 7: A Summary of Important Topologies.